Chem

CellPress

Article

Experimentally Modeling the Emergence of Prebiotically Plausible Phospholipid Vesicles

Sunil Pulletikurti,[1, 2, 5] Kollery, S. Veena,[1, 2, 5] Mahipal Yadav,[1,2] Ashok A. Deniz,[1, 3] * and Ramanarayanan Krishnamurthy[1, 2, 4] *

[1] The Scripps Research Institute, 10550 North Torrey Pines Rd, La Jolla, CA 92037, USA

[2] Department of Chemistry,

[3] Department of Integrative Structural and Computational Biology

[4] Lead contact

[5] The authors contributed equally

* Correspondence: deniz@scripps.edu; rkrishna@scripps.edu

Dedicated to the memory of Professor Albert Eschenmoser

SUMMARY

The prebiotic emergence of protocells is an important part of any origins of life scenario. While fatty acid-based vesicles are well studied, how they transitioned to phospholipid vesicles is uncertain. Herein we show that cyclic-phospholipids formed from fatty acids and glycerol could have played a role by generating a heterogeneous library of vesicles with diverse morphologies and tolerance to a range of metal ions, temperature and pH. The cyclic phosphate moiety facilitates the natural emergence of vesicles composed of diacyl-phospholipids to become part of the chemical evolutionary process. Competing emergent properties of the various systems (facilitated by additives) could have led to an early preference of the sn-1,2-acyl-substitution on the glycerol backbone coincidental with extant biology. Thus, cyclic-phospholipids could have played a significant role not only in early prebiotic protocellular chemistry but also in facilitating the chemical evolution of protocells from the structurally simple to the functionally more complex.

Fatty acids, Glycerol, Protocells, Cyclic-phospholipids, Diacyl phospholipids, Vesicles

INTRODUCTION

The formation of membranous and vesicular structures are proposed as important intermediary steps towards the emergence of protocells in the chemical evolutionary processes leading to origins of life on early Earth.[1-4] In that context, prebiotically plausible short chain fatty acids (e.g., carbon chains of C9 – C12) have been proposed as the most realistic candidates and shown to form vesicles of

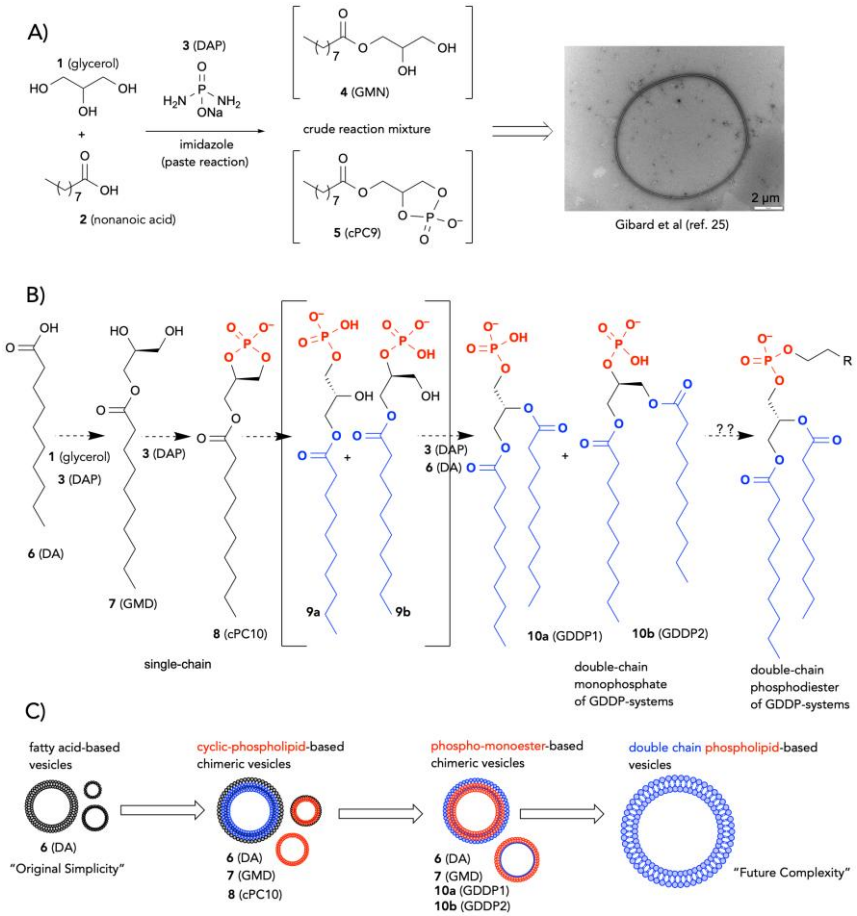

Figure 1. Cyclic-phospholipid based scenario for the emergence of phospholipid vesicles. (a) Plausible prebiotic synthesis of cyclic-phospholipids starting from fatty acids and glycerol mediated by phosphorylation with diamidophosphate (DAP). (b) A proposed pathway of molecular transformations starting from fatty (decanoic) acid mediated by DAP and glycerol giving rise to cyclic-phospholipid cPC10. The hydrolysis of the energetic cyclic phosphate moiety is proposed to lead to the transient formation of single chain monophosphate lipids that on subsequent esterification with DA would form double-chain monophosphate lipids. Further esterification of the monophosphate would provide the double chain phosphodiesters. Note: we show the chirality of the compounds that were synthesized and used in this study and do not imply any chiral selection in the first step. (c) This series of transformations at the molecular level is suggestive of corresponding series of hypothetical transitions at the supramolecular level (of vesicles): the vesicles composed of simple fatty acid (DA) are proposed to be transformed by stepwise incorporation of (its products from the phosphorylation reaction) the glycerol ester, GMD and/or single chain cyclic-phospholipid (cPC10). This mixing is hypothesized to give rise to vesicles composed of mixtures (chimeric vesicles) based on cyclic-phospholipid (e.g., DA:cPC10 or GMD:cPC10). The subsequent transformation of the cyclic-phospholipid (via **9a** and **9b**) to form GDDP1 and GDDP2 is expected to transform the cPC-based vesicle-system to the next level of vesicles based on phosphomonoester double chain-based phospholipids which have the potential for further esterification at the phosphate moiety and for the emergence of double chain phosphodiester-based vesicles. GMN = glyceryl mono-nonanoate. cPCX: cP refers to cyclic Phospholipid and CX refers to the carbon chain length of the fatty acid (C9, C10 etc.). Red color in Figure 1C refers to cyclic-phospholipid or phospho-mono/di-ester lipids present in the vesicle. Blue color in Figure 1C refers to double-chain phospholipids present in the vesicle. The mixture of color-layering represents the mixed (hybrid) composition of vesicles.

homogeneous compositions capable of limited encapsulation, growth and division.[5] However, these homogeneous short chain fatty acid vesicles have some disadvantages in terms of a narrow range of function and stability – for example, in terms of pH, temperature and metal ion concentrations – compromising their potential further development.[6] Therefore, inclusion of other prebiotically plausible molecules (available from extraterrestrial sources such as meteorites or from reactions on early Earth geochemical environments) as additives such as the corresponding short chain fatty alcohols, and/or the respective mono-glyceride esters, or other

small molecules -resulting in heterogeneous vesicle compositions- have been investigated and shown to provide relief to many of these shortcomings.[6-10] For example, a system based on mixed decanoic acid and its corresponding mono-glyceride ester have been shown to have advantages with respect to stability to metal ions. And the presence of amino acids and nucleobases have been demonstrated to contribute to the stability of these decanoic acid-based vesicles.

As successful these studies have been, these do not address the question of roles played by the emergence of (and transition to) phospholipid derivatives that extant life is based on.[11] In fact, it has been argued that amphiphilic molecules resembling contemporary phospholipids were unlikely to be available for the first forms of cellular life and that the first membranes assembled spontaneously from simpler amphiphilic compounds that were available in the prebiotic environment.[1]

Nevertheless, there are some examples considering phospholipids in a prebiotic context[12-15], and recent work documenting the behavior of long chain phospholipids mixed with fatty acids[16-18]. For example, Deamer group's pioneering work showed the prebiotic synthesis of phospholipids and subsequent formation of membrane structures starting from glycerol and n-dodecanoate in the presence of dicyanamide and phosphate.[12] Fiore and Strazewski have synthesized monoalkyl phosphates and their corresponding ethanolamine derivatives, which were shown to form giant vesicles while Bonfio et al have shown that glycerol-2-phosphate can be acylated with short chain fatty acids to form a library of acylglycerol phosphates that self-assemble to form stable vesicles.[13,15] In spite of such studies, there is a general opinion that long-chain phospholipids are later descendants presumably from biological pathways.[1] And, there are some studies investigating the vesicle forming properties of single chain alkyl phosphates, which showed the scope and limitations of single chain phosphates in their propensity for vesicle formation at ambient conditions, such as near neutral pH.[13,19,20] Therefore, the primary focus continues to be on membranes derived from short chain fatty acids[21] and mixtures derived from corresponding alcohols and glycerides, largely devoid of (short chain) phospholipid derivatives[22,23], leaving open the conceivable routes by which prebiotically plausible short chain phospholipids can get involved in the process of chemical evolution of protocells.[14,18,20,24]

We became interested in the role of short alkyl chain phosphoglycerides in protocell/vesicle formation based on the discovery that a one-pot prebiotic phosphorylation of a mixture of short chain fatty acid and glycerol yielded single-chain cyclic-phospholipids (cPCs), which enabled the formation of vesicles in the same reaction milieu (Figure 1A).[25] Furthermore, though cPCs themselves could form vesicles (e.g., cPC9, high concentrations, ca 350 mM)[25], it was shown that the combination of fatty alcohols, glyceryl monodecanoate (GMD) and cPCs produced vesicles at much lower concentrations (20 mM), are more robust to a range of pH and divalent metal ions, and in retaining negatively charged biological and small molecules, when compared to their corresponding fatty acid derived counterparts.[26] Moreover, we observed that the cPCs could be selectively hydrolyzed to form the regioisomers of the corresponding single-chain GMD-monophosphates.[27] These experimental observations led us to hypothesize (Figure 1B and 1C) that the concurrent prebiotic formation of cPCs from fatty acids and glycerol and their incorporation into primitive fatty acid-based vesicles could play a role in facilitating the chemical evolution of primitive vesicles ('original simplicity') into protocells already having the innate potential to transform to double-chain phospholipids ('future complexity')[28] as depicted in Figure 1C. The ring opening of these 'high-energy' five-membered cyclic phosphates followed by (concomitant) esterification reaction with fatty acids would be central to this hypothetical scenario.

Accordingly, we chose to experimentally model such a transition by investigating the role of these single-chain cPCs and their corresponding double-chain phosphate derivatives in the context of vesicles derived from fatty acids and their corresponding glyceride derivatives. In this context, the selection of systems was motivated by (a) the types of compounds potentially generated by the prebiotic phosphorylation of a mixture of glycerol (**1**) and nonanoic acid (**2**, NA) by diamidophosphate (**3**, DAP) shown in Figure 1A and (b) the widely studied decanoic acid (**6**, DA) and glyceryl monodecanoate (**7**, GMD) based systems.[6,25,29,30] The reaction components and its chemical reactions in Figure 1A allow, in theory, also for the double-chain GDDP systems **10a** (GDDP1, glyceryl 2,3-didecanoate 1-phosphate) and **10b** (GDDP2, glyceryl 1,3-didecanoate 2-phosphate) to form. Since we were following this sequence of events (Figure 1B) we did not consider the role of (a) fatty alcohols and (b) the corresponding phosphodiesters of GDDP in this investigation. For this proof-of-principle demonstration, thus, we chose to investigate the binary-mixtures derived from cyclic-phospholipid of GMD (**8**, cPC10) and the corresponding decanoic acid DA **6**, GMD **7** and the phosphorylated glyceryl didecanoates (**10a**, GDDP1 and **10b**, GDDP2) shown in Figure 1B. Our focus was on mapping the landscape of vesicles stemming from the cPC10-based systems leading to emergent

properties, and not on finding an "optimal" protocell that could harbor one type of reaction scenario.

Herein we report on the vesicle forming properties of these heterogeneous binary-mixtures and compare their behavior with their fatty acid counterparts. Our observations show that, even at the C10-level, there is a range of morphologically diverse and robust vesicles that are formed from prebiotically plausible mixtures generated from decanoic acid, its glycerides, the corresponding and double chain-cyclic-phospholipid derivatives. Such an observation provides support for a systems chemistry model that includes a spectrum of prebiotically plausible phospholipids from the very beginning as components of early protocells in a systems chemistry setting – and, therefore, harbor the potential to provide continuity and transition towards extant cells composed primarily of phospho-(diester)-lipids.

Choice of binary systems for vesicle studies. In order to limit the chemical space of mixed composition of vesicles we focused on binary mixtures in the decanoic acid series. On the basis of our previous work[25] and the hypothesized natural emergence of products in Figure 1B, we identified at the first level, three possible binary mixtures of (a) decanoic acid **6** with GMD **7**, (b) decanoic acid **6** with cPC10 **8** and (c) GMD **7** with cPC10 **8** that can be used to generate vesicles. Since the binary combination of **6** and **7** has been extensively studied[23,30-32], we focused on investigating the propensity of vesicle formation with binary mixtures from cPC10 **8** with **6** and **7**.

For the next level of binary systems based on Figure 1B, we considered the products **9a** and **9b** produced by the hydrolysis of the cyclic phosphate moiety of cPC10 (Figure 1B). This was based on the previous observation that cPC10 **8** is hydrolyzed selectively at the cyclic phosphate moiety and gives rise to a mixture of single chain phospholipids **9a** and **9b**.[27] This allowed us to postulate a hypothetical scenario (Figure 1B) where further esterification of these single chain phospholipids **9a** and **9b** could give rise, eventually, to the double chain phospholipids GDDP1 **10a** and GDDP2 **10b** (by the same type of DAP mediated esterification process observed in Figure 1A). Single chain phosphates similar to **9a** and **9b** have been shown to need highly acidic pH (≈2) to form vesicles[19], and more recently it has been shown that **9b** does not form vesicle like structures under near neutral pH conditions.[15] Therefore, we excluded **9a** and **9b** from this study, as we aimed to keep (a) the pH range from 4-8 thought to be conducive for many prebiotic scenarios and reactions[33-35] and (b) the focus on its diacyl derivatives **10a** and **10b**. Thus, we chose two possible binary mixtures derived from the double-chain phosphates **10a** and **10b**: (a) GMD **7** with GDDP1 **10a** and (b) GMD **7** with GDDP2 **10b** which would be phospholipid counterparts to the well-known decanoic acid-GMD studies in the literature. All of the compounds derived from the decanoic acid series (Figure 1B) were synthesized based on procedures described in the literature (see SI for details) starting from decanoic acid and (*R*)-(2,2-dimethyl-1,3-dioxalan-4-yl)methanol.[27]

Experimental Approach: Vesicles were prepared modifying the procedure we developed in our previous work.[26] We started either from the solutions/suspensions of the individual components in the buffer of choice or from mixing the individual components as solids and adding the desired buffer. Sonication, followed by short heating-cooling cycles and equilibration overnight with shaking (see SI for details) afforded the samples that we analyzed further.

Since the critical aggregate concentration (CAC) was expected to change with varying binary compositions and pH, we used confocal microscopy and brightfield images employing various fluorescent dyes, primarily rhodamine 6G (R6G) along with AF488-dextran10 kDa and Cyanine5 carboxylic acid (Cy5), to visually inspect and judge vesicle formation as this was deemed more reliable for our purpose. Brightfield images were used to distinguish between vesicles and droplets.[36] We examined different regions of the same sample and also from different trials to ensure reproducibility of the presence or absence of vesicles. Depending on the systems studied and the conditions under which they were formed, the number of vesicles ranged from a plethora to a few to none. In many of the systems studied here we observed a variety of heterogeneous mixtures of co-existing vesicle types made up of bilayer membranes, undefined shapes and aggregates etc. The various vesicles types were determined by visually inspecting the fluorescent dye-labeled confocal images and classifying them based on their appearance (e.g. circularity and the number of membranes) following the terminology described by Walde et al[37] – such as the lamellarity [the number of the layer of membranes in a vesicle, unilamellar vesicles (ULV); oligolamellar (OLV); multilamellar (MLV); multivesicular (MVV)], aggregated vesicles (touching each other) and vesicles that share a section of the membrane. In cases where the fluorescent dye-labeled images of vesicles were not clear, the type and lamellarity was confirmed by visualization through brightfield images in confocal microscopy. Furthermore, the formation and presence of vesicles were corroborated by performing (a) a confocal z-stack profile of fluorescently labeled structures to visualize the three-dimensional shape along with the lacuna and (b) by encapsulation and leakage studies using AF488-dextran 10 kDa.

To determine the optimal ratio of the binary mixture for vesicle formation we initially chose a total concentration of 40 mM and a pH range of 6-7 (usually around 6.5). The pH range was determined by the pKa of decanoic acid (6.4)[38,39] and the fact that the cPC10 (pKa ≈ 2) and double-chain phospholipids (pKa ≈ 2 and 6.5 corresponding to the two ionization states of the monoalkyl-phosphate group) are going to be mostly in the deprotonated state in the plausible prebiotic pH range (4-8) under consideration. In certain cases, we also varied the pH and the ratios of the components to understand the effect of change of pH on the vesicle formation with changing composition. We also looked at the effect of heating-cooling protocols that are generally used in vesicle preparation (to get the fatty acids into solution). Once we settled on a particular method, ratio of the binary mixture and the pH, we investigated the effect of metal ions and temperature on the stability and the robustness of the vesicles using R6G and in select cases with AF488-dextran 10 kDa. Experiments were run in duplicate to check the reproducibility of the results. Since the cPC10 and the GDDP molecules are not commercially available and have to be synthesized, we had to make judicious choices about the types and number of experiments we could run. For example, as in the leakage assays which necessitated large volumes of running buffers containing these molecules for purification and isolation of vesicles by size-exclusion chromatography.

RESULTS

Cyclic-phospholipid (cPC) based heterogeneous systems form a variety of giant multilamellar (MLV), oligolamellar (OLV), multivesicular (MVV) and unilamellar (ULV) vesicles that coexist with other structures.

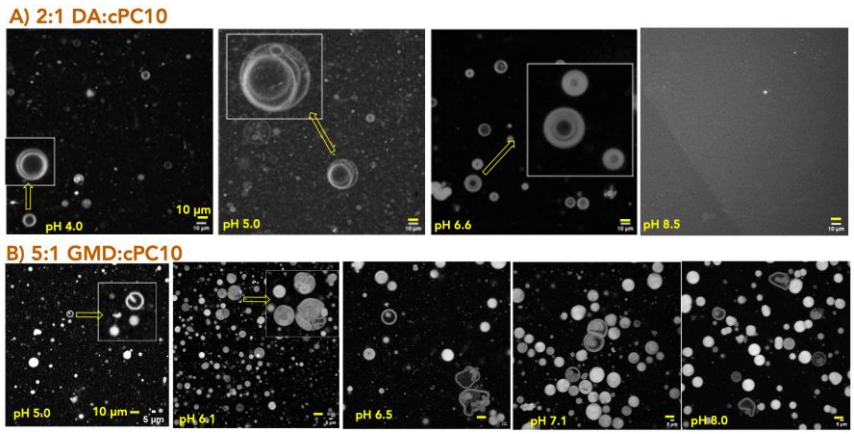

Figure 2. Change in pH leads to different morphological shapes in vesicles generated from 2:1 DA:cPC10 and 5:1 GMD:cPC10 systems. Confocal microscopy images of cPC10-based vesicles (total concentration 40 mM) as a function of pH (A) 2:1 DA:cPC10 (24 h) and (B) 5:1 GMD:cPC10 (18-21 h). Vesicles are labeled with R6G. Inset: Expansion of the pointed area. Yellow scale bars represent 10 µm as indicated above. For more information see SI (Figure S2 for 2:1 DA:cPC10; S16 for 5:1 GMD:cPC10).

cPC10 based systems - decanoic acid **6** with cPC10 **8** and GMD **7** with cPC10 **8:** We first studied a series of ratios and pHs and observed that the ratios of 1:1, 2:1 and 5:1 DA:cPC10 formed MLVs and ULVs at pH ca. 6.5 (Figure S1). Moreover, the 2:1 DA:cPC10 system was found to have good vesicle structure and stability over a range of pH 4.0-6.6 as seen by confocal images (Figure S2), which led us to select this binary system for further studies. Increasing the pH in the 2:1 series resulted in a transition from ULVs (pH 4.0) to MVVs (pH 5.0) to OLVs and MLVs (pH 6.6) – suggesting that the various degrees of protonated forms of DA (pKa 6.4) are providing the necessary hydrogen-bonding (with the completely ionized cPC10, pKa ≈ 2) and along with charge repulsion effects – are primarily responsible for the different morphologies of the vesicles (Figure 2A). As expected, based on charge-repulsion effects, at pH 8.5 the combination of the two negatively charged decanoate and cyclic phosphate did not form vesicles. While decanoic acid alone did form vesicles around pH 7.5 and above, it formed more undefined shapes from pH 5.0-6.5 consistent with previous studies (Figure S1).[40,41]

In the GMD **7** + cPC10 **8** series we used pH 6.1 and 40 mM total concentration as a starting point to screen the ratio of the two components and observed vesicle formation starting from a ratio of 2:1 GMD:cPC10 onwards with a 5:1 and 7:1 ratio and exhibiting a greater abundance of heterogenous vesicles composed of bilayer membranes coexisting with amorphous aggregated vesicles (Figure S15). We chose the 5:1 system to investigate further which formed vesicles robustly over a pH range of 6.1-8.0 over a period of days (Figure

S16). And as in the previous case, the lower pH of 6.1 produced a greater proportion of ULVs and MVVs with many nested smaller vesicles within larger (> 20-25 micron) vesicles, while the higher pH (7.0-8.0) tend towards a distribution containing more MLVs coexisting with other structures such as aggregated vesicles and vesicles that share membrane sections (Figure 2B). This transformation was also observed by confocal microscopy as the pH of the samples was adjusted in real time from 6.2 to 7.2 (Figure S18). Though vesicles were formed at concentrations as low as 5 mM the ones formed at 40 mM were found to have a greater degree of persistence over time (Figure S19). And starting from either pure component GMD **7** or cPC10 **8** at pH 6.1 (which were appearing as amorphous shapes) the addition of the corresponding percentage of the other component (16.6% of **8** or 83.3% of **7** respectively) led to relatively rapid (within 30 min.) formation of vesicles as observed in real-time by confocal microscopy (Figure S21). The CAC of these DA:cPC10 based systems was in the range of 5-13 mM whereas the GMD:cPC10 based systems was around 1.5 mM (Table S1, S2) compared to the 10 mM reported for cPC10 alone[26,42]. The lowering of the CAC in these hybrid systems is consistent with previous reports.[26,42] Our results so far suggest (a) enhanced vesicle stabilization in these hybrid cPC10 systems, and (b) dependence of vesicle formation and morphology on solution conditions such as pH – consistent with physicochemical characteristics of these systems. We next proceeded to probe these heterogeneous vesicles in greater detail.

Heating-cooling cycles control the structure and morphology of the cPC10 **8** containing vesicles producing a mixture of thick-walled MLVs and OLVs: While evaluating various literature protocols[37,43-46] (Section 2 in SI) for preparing the cPC10 containing vesicles we observed that heating (used to obtain a uniform suspension or solution of the vesicle components) seemed to affect the size, type and quality of the vesicles formed (Figure 3, Figure S3-S5, S20-S21), with short heating-cooling cycles producing giant MVVs, OLVs and MLVs.

When the 2:1 DA:cPC10 vesicles at pH 6.5 were subjected to post warming-cooling (50-60°C to 35°C) protocols, giant multilamellar and oligolamellar vesicles (MLVs and OLVs) were formed robustly, a phenomenon that was accentuated by warming for longer times (Fig S4-S5, Videos S1-S3). For example, when the initially formed vesicles were heated to 60°C (10-15 min) and cooled to 35°C (20 min) it resulted in the formation of giant ULVs and MLVs (Figure S5). When we used AF488-labeled dextran to monitor the effect of the heating (60 °C)-cooling (35 °C) protocol we observed images that showed GUVs (giant unilamellar vesicles) as well as remodeling of the vesicles to MVVs (Figure 3C, Figure S4). In some cases, during the heat-cool induced transition process, we also observed that the AF488-dextran dye had become concentrated also in the membrane bilayers (Figure S4) – a phenomenon that was not expected, but not uncommon as some water-soluble dyes are known to interact with lipid bilayers.[47] This allowed us to observe the spherical shape of the MVVs and its lumen containing the smaller vesicles via a z-stack image (Figure 3C, Videos S4-S6).

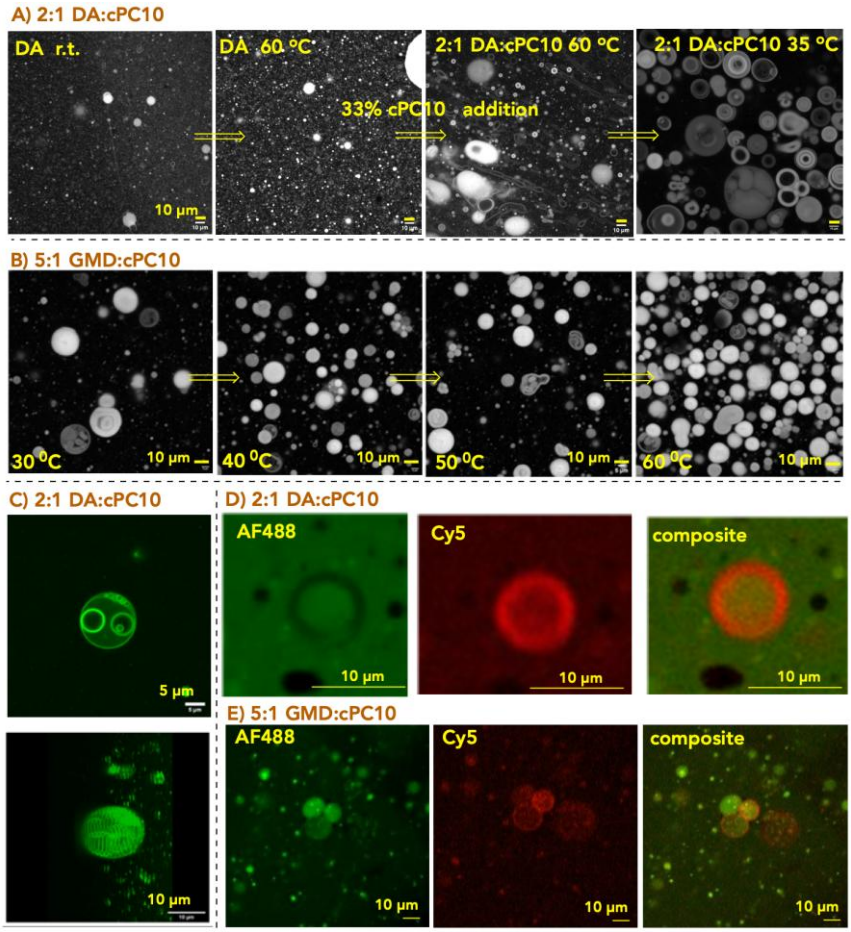

Figure 3. Comparison of the effect of temperature on the vesicles generated from 2:1 DA:cPC10 versus 5:1 GMD:cPC10 by monitoring in real-time by confocal microscopy and by use of fluorescent dyes.
Confocal microscopy images of cPC10-based vesicles (total concentration 40 mM) as a function of temperature (heating-cooling) in the confocal microscope instrument: (A) DA, labeled with R6G, pH 6.6 was heated to 60 °C and then 33% of cPC10 was added (as a stock solution from 40 mM stock solution) at 60 °C and cooled to 30 °C. (B) 5:1 mixture of GMD and cPC10, labeled with 0.04 mM R6G was imaged in real time at different temperatures while heating to 60 °C. (C) 2:1 DA:cPC10, labeled with 0.02 mM AF-488 dextran 10 kDa, purified by spin-column and imaged after one heating-cooling cycle (30-60-30 °C, total duration of 40 min). (D) 2:1 DA:cPC10, labeled with 0.01 mM Cy5 carboxylic acid and 0.02 mM AF-488 dextran 10 kDa (imaged 2 hours after preparation without purification) – please see Figure S6 and captions for further details. The scale bars represent 10 µm and 5 µm as indicated above. (E) 5:1 GMD:cPC10 labelled with 0.08 mM Cy5 carboxylic acid and 0.02 mM AF-488 dextran 10 kDa at pH 5.0 (168 h). For more information see experimental section in SI (Figure S4, S6 for 2:1 DA:cPC10; Figure S21, S29 for 5:1 GMD:cPC10).

Realtime observation by confocal microscopy showed the dynamic, accelerated and robust vesicle formation during the heat-cool process: Under the heating conditions the DA-based vesicles underwent a phase transition around 40°C and formed oil droplets (up to 60 °C) and did not reorganize into any observable vesicle like structures on cooling (Figure S4). In another experiment, we started with pure DA (using R6G dye) and heated it to 60 °C and then added 33% cPC10 (from stock solution) to make the 2:1 DA:cPC10 mixture in situ. Monitoring this heterogeneous system by confocal microscopy over an hour showed the appearance of tube-like structures which seemed to grow that led to the formation of giant MVVs during the cooling process (Figure, 3A, Figure S4) – corroborating the observations when we started with the 2:1 DA:cPC10 mixture from the beginning (Figure S1).

The vesicles, thus generated by these heat-cool process, were found to be robustly stable over period of days and on many occasions exhibited dynamic behavior of division or fusion as observed by confocal videos (Videos S4-S15). Vesicle formation was confirmed by obtaining 3-D images ("z-stack") by confocal microscopy and by the use of a combination of the

membrane-labelling dye Cy5 and the hydrophilic dye AF488-labeled dextran for encapsulation (Figure 3C-3D, Figure S6, Video S14-S15). Both of them clearly show the lumen of the vesicle corroborating the confocal images obtained by using the membrane labeling R6G dye alone.

The 5:1 GMD:cPC10 system formed MVVs and MLVs robustly via the heating-cooling protocols employed in their preparation (Figure S17-20). And when they were subjected to heating to 60 $^{\circ}$C they maintained their structural integrity while producing more MLVs (Figure 3B, Figures S21). A big difference when compared to the DA:cPC10 system was the ubiquitous formation of giant unilamellar vesicles that encapsulated many other ULVs and/or MLVs (Figure S21).

Our studies thus far demonstrate that the presence of cPC10 contributes to stability in mixed systems either with DA or GMD. Furthermore, our results suggest a somewhat higher stability of the GMD:cPC10 vesicles when compared to DA:cPC10 systems. This result is consistent with the charge-neutral character and hydrogen bonding capability of GMD stabilizing membrane formation with the negatively charged cPC10, also in keeping with the lower CAC noted above. We also note that strikingly, progress along the proposed chemical evolution pathway (Figure 1) from DA through GMD to cPC10 results in more stable mixed vesicles. It is plausible that such an increased stability could also drive reaction progress in this chemical evolution pathway by mass action or other physicochemical mechanisms potentially including a positive feedback loop in a systems chemistry context.

Presence of cPC10 increased the tolerance of vesicles to metal ions when compared to DA (Figure 4): Next, the effect of metal ions on these cPC10-containing vesicles were probed. Previous observations have shown that vesicles formed from cPC10 (negatively charged molecule) and dodecanol (a neutral molecule) had a better tolerance for Mg^{2+} salts as compared to those from DA:dodecanol.[26] Given the low pKa of ≈ 2 of cPC10 and the higher pKa of 6.4 DA, the role of pH and the valency of the metal ions were expected to have differing effects between the DA:cPC10 (charged:charged) system versus the GMD:cPC10 (neutral:charged) system – based on the varying state of ionization of DA, valency of metal ions, screening of charge repulsion, degree of hydration/dehydration etc. At pH 6.6, the 2:1 DA:cPC10 vesicles were stable to the presence of monovalent (Na^+ and K^+) salts up to 0.8 M NaCl and 2.0 M KCl (Figure 4A), with flocculation and amorphous structures appearing at 1.2 M NaCl (Figures S7). In the case of divalent metal ions, up to 25 mM Mg^{2+} and Ca^{2+} were tolerated while higher concentrations of these metal ions led to flocculation/aggregation and nebulous shapes (Figure 4A, Figures S8). The use of synthetic sea salt which has a combination of monovalent and divalent metal ions showed the presence of the vesicles up to a concentration of 166 mM Na^+, 20 mM Mg^{2+}, 2 mM Ca^{2+} and 2 mM K^+ beyond which the vesicles were destroyed (Figure 4A, Figure S10). Furthermore, we observed that the vesicles (beginning at 10 mM Mg^{2+}) were morphing their shape, the thickness of the 'membranes' and lamellarity in response to increasing concentrations of Mg^{2+} (Figure S11-S12). This was also true in the case of K^+ ions where higher concentrations resulted in more unilamellar vesicles (Figure S11) - implying these counterions can affect not only the stability of the vesicles but also control their morphological appearance.[31,48]

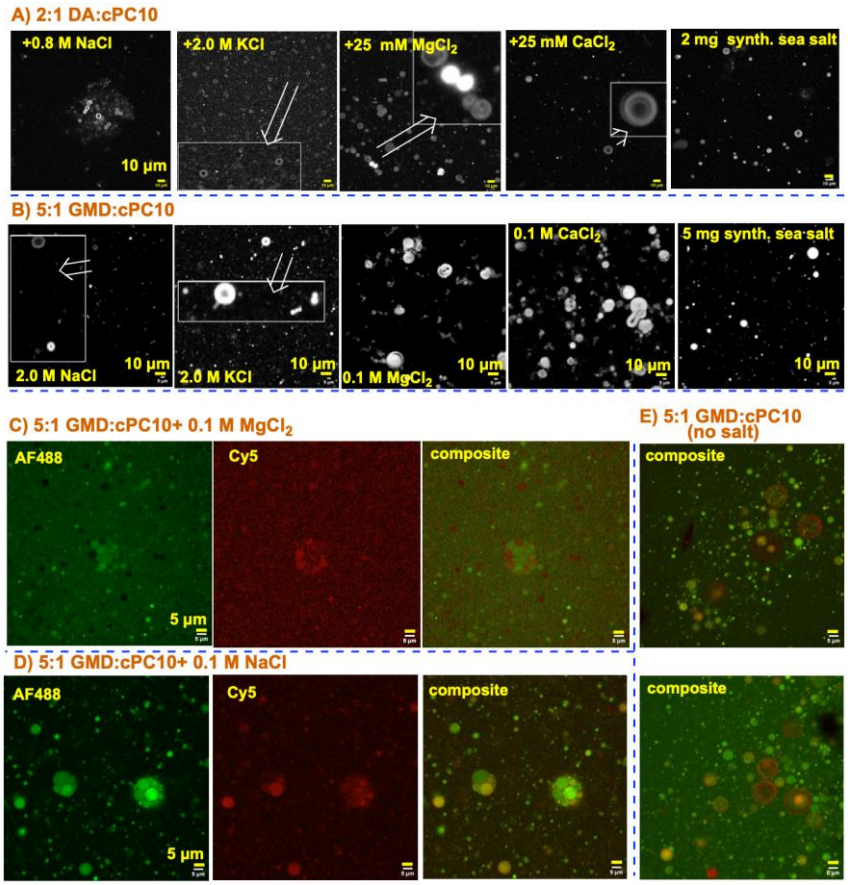

Figure 4. Comparison of the effect of metal ions on the vesicles generated from 2:1 DA:cPC10 versus 5:1 GMD:cPC10 by use of fluorescent- dyes. Confocal microscopy images of cPC10-based vesicles (total concentration 40 mM) labeled with R6G in the presence of various metal ions generated from of (A) 2:1 DA:cPC10, pH 6.6 (24 h) and (B) 5:1 GMD:cPC10, pH 6.3 (72-120 h). Confocal microscopy images of vesicles generated from 5:1 GMD:cPC10, pH 5.0 labelled with 0.08 mM Cy5 carboxylic acid and 0.02 mM AF-488 dextran 10 kDa (C) in the presence of 0.1 M Mg^{2+} (168 h). (D) in the presence of 0.1 M NaCl (168 h) (E) No salt (168 h). Inset: Expansion of the pointed area. Synthetic sea salt (1 mg in 130 µL of sample volume) contains 83 mM Na^{+}, 10 mM Mg^{2+}, 1 mM K^{+}, 1 mM Ca^{2+}. The scale bars represent 10 µm and 5 µm as indicated above. For more information see SI (Figure S7-10 for 2:1 DA:cPC10; S24-29 for GMD:cPC10).

A similar effect of the divalent metal ions and synthetic sea salt was observed with the corresponding 2:1 DA:GMD vesicles at pH 6.5 which survived up to 25 mM of Mg^{2+} or Ca^{2+} salts (Figure S9) while vesicles from DA alone was precipitated out by 1 mg of synthetic sea salt (that has 10 mM of Mg^{2+} and 1 mM of Ca^{2+}, Figure S10). And as was seen with the cPC10:dodecanol systems, the presence of Na^{+} provided a higher tolerance for Mg^{+2} concentrations (Figure S12) which was not the case for DA, which under identical conditions formed amorphous shapes (Figure S12).

These results are striking considering the fact (a) that these divalent metal ions tend to cause precipitation[49,50] (b) that the DA:cPC10 (two negatively charged species) combination is almost approximating the behavior of DA:GMD under identical conditions. And heating in the presence of the cations (1.2 M of Na^{+} and K^{+}) caused flocculation and aggregation of vesicles by 24 hours. In the presence of up to 10 mM divalent Mg^{2+} a similar heating protocol resulted in morphological changes (remodeling) of the intact ULVs while higher Mg^{2+} concentrations caused aggregation/flocculation (Figure S11).

GMD:cPC10 systems were more stable with divergent responses to monovalent and divalent metal ions when compared to DA:cPC10 systems: There was remarkable difference when it came to the effects of the monovalent versus divalent metal ions in the case of the vesicles generated from the GMD:cPC10 system (Figure 4). Increasing concentrations of both the monovalent ions Na^{+} or K^{+} led to decrease in the size, multi-lamellarity and number of the vesicles both at pH 6.2 and 5.0 (Figure S24), whereas increasing concentrations (up to 50 mM)

of divalent metal ions Mg^{2+} or Ca^{2+} had little impact on GMD:cPC10 vesicles (Figure S25). Further increase to 75-100 mM of Mg^{2+} or Ca^{2+} did result in remodeling of the vesicles along with change in lamellarity and morphology; in addition, some flocculation had taken place. However, diluting the sample back to 50 mM of the metal ion restored the GMD:cPC10 vesicles to their original multilamellar nature (Figure S27). The integrity of the vesicle structure at high divalent metal concentration (0.1 M Mg^{2+}) was shown by the use of dyes Cy5 and Alexa-448 labeled dextran 10 kDa where both dyes showed that the structure of these vesicles had not been compromised (Figures S28-S29). The use of synthetic sea salt even at higher concentrations (390 mM Na^{+}, 43 mM Mg^{2+} and 8.3 mM Ca^{2+}) or heating in the presence of metals also did not disrupt the GMD:cPC10 vesicles (Figures S25 and S26).

The stability of these GMD-cPC10 vesicles with respect to high Mg^{2+} salt concentrations even at the short chain (C10) level is significant when compared to the reported[49,50] stability observed for blended long chain (C18) oleic acid/-palmitoyl-2-oleoyl-sn-glycero-3-phosphocholine (POPC) membranes. These observations, not surprisingly, are different when compared to that of the vesicles formed by the DA+cPC10 system. Since GMD has a 1,2-dihydroxyl moiety which could act as chelator[51] of the divalent metal, it is plausible that the act of chelation could cause a change in morphology of the vesicles – by holding these divalent

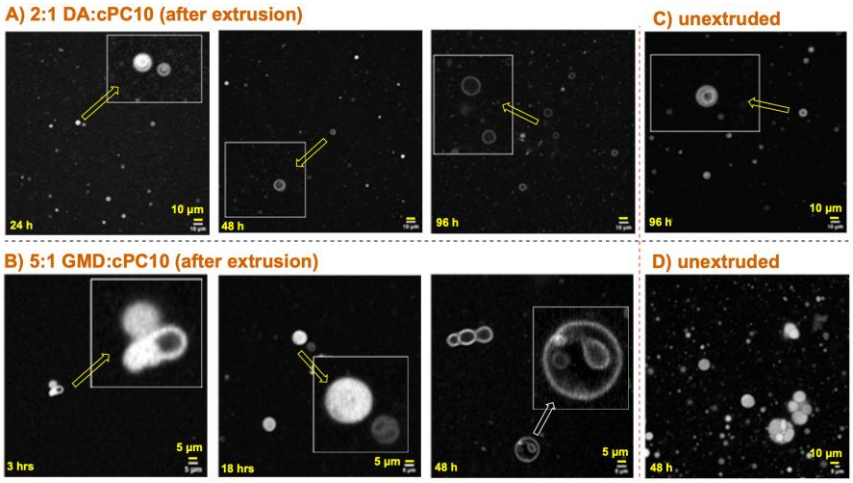

Figure 5. Extrusion of vesicles from 2:1 DA:cPC10 versus 5:1 GMD:cPC10 system result in giant unilamellar vesicles (GUVs) that are stable over time. Effect of extrusion on the cPC10-based vesicles (total concentration 40 mM). Confocal microscopy imaging of the 40 mM of (A) 2:1 DA:cPC10, pH 6.6 (B) the 5:1 GMD:cPC10, pH 6.3 as a function of time. The samples were labeled with R6G and extruded 11 times through 0.4 µm polycarbonate membrane. (C) and (D) are the corresponding unextruded control in the 2:1 DA:cPC10 and 5:1 GMD:cPC10 series respectively at comparable times. The scale bars represent 10 µm and 5 µm as indicated above. For more information see SI (Figure S14 for 2:1 DA:cPC10; Figure S22 for 5:1 GMD:cPC10).

metal ions close to the negatively charged cPC10 **8**; and this in turn, by the interaction of the ions with water molecules, could cause changes by swelling of water layers between the bilayers[52] leading to the morphological changes. And the increasing stability observed here is also in consonance with the previous observations of increased stability of GMD containing fatty acid vesicles to divalent metal ions as opposed to pure fatty acid vesicles.[32] The corresponding 5:1 GMD:DA system also formed vesicles but with smaller dimensions and the addition of divalent metal ions led to a decrease in the number of the vesicles along with appearance of indistinct structures/shapes (Figure S30). Thus, our ion-dependence studies provide additional support for the idea that the combination of GMD+cPC10 seems to generate more robust and persistent vesicles when compared to the ones generated from the DA+cPC10 system. This is also true for the synthetic sea salt studies (Table S5). GMD alone under these conditions did form relatively smaller "vesicle like" structures an observation consistent with previous reports and were affected minimally with presence of metal ions and change in pH (Figure S31).[6,32,53]

cPC10 containing vesicles extruded through 0.1-5 micron polycarbonate membranes show 'growth' (increase in vesicle size) over time leading to re-forming giant vesicles (Figure 5): For most of the studies described above the cPC10 containing heterogeneous vesicles were generated as is by the simple mixing of their individual components. However, in many of the previous works, the vesicles are subjected to a final extrusion processing step through a

polycarbonate membrane to generate homogeneous and/or unilamellar vesicles.[54] The rapid movement of the lipids caused by the extrusion process is thought to lead to a thermodynamically more stable state quicker than the undisturbed cases where there is a slow movement of lipids. Therefore, to understand the effect of such extrusion process on the cPC10 containing vesicles, we subjected the vesicles generated by the above-described procedures to extrusions (11 times) through the polycarbonate membrane and monitored by confocal imaging as to how they behaved over time.

Extrusion of the 2:1 DA:cPC10 heterogeneous system through a 0.4 micron polycarbonate membrane gave rise to mostly uniform unilamellar vesicles (Figures S13-S14) with correspondingly smaller sizes (1-2 microns) within 3 hours. With time (24-72h) they formed larger vesicles (2-10 microns) as also seen by the change in size-distribution graphs over time and eventually matched the sizes seen in the unextruded sample – suggesting the increase in vesicle sizes over time. Furthermore, the size and lamellarity differed depending on the pH, with pH 5.0 showing more ULV and MVV character while pH 6.5 exhibited more MLV attributes – indicating that there is a tendency for the 2:1 DA:cPC10 to grow to a certain size with particular morphology depending on the conditions.

The initially prepared giant vesicles derived from 5:1 GMD:cPC10 were subjected to extrusion through various polycarbonate membranes (0.1, 0.4 and 5 microns) and were observed to reform the giant vesicles over time – with the 0.1 and 0.4 microns forming more ULVs in comparison to the 5 micron membrane (Figure S22). The vesicles derived from 5:1 GMD:cPC10 seemed show more resilience to the extrusion process as evidenced by the presence of bigger vesicles (avg 5 microns) even at 3 hours and growing over 48 hours (Figure S22). This behavior is similar to those observed with the vesicles formed from the DA **6** with cPC10 **8** system and seems to suggest that the presence of cPC10 may be the determining factor – since such a robust re-growth (increase in vesicle size) behavior was not observed with the corresponding 5:1 GMD:DA system (Figure S23).

Such increases in vesicle size over time after extrusion have been observed before in other homogeneous systems.[55-57] This growth-after-extrusion behavior has been attributed[56] to (a) the possibility that immediate average sizes obtained by forced extrusion may not reflect the thermodynamic stable size/state and (b) vesicle growth (i.e., increase in vesicle size) by fusion may occur over time due to energy available at the equilibration conditions afterwards. In the cPC10-based heterogenous systems there may be an added factor at play – that is the vesicles' compositional heterogeneity (such as population imbalance of DA, GMD and cPC10) that can cause growth by incorporation of components[16,58] (related to point (a) above).

GMD:cPC10 vesicles are able to encapsulate and retain AF488-dextran 10 kDa better than DA:cPC10 vesicles (Figure 6): In order to assess the stability of these 2:1 DA:cPC10 and 5:1 GMD:cPC10 vesicles we prepared the AF488-dextran 10 kDa encapsulated vesicles and isolated them by size-exclusion chromatography (SEC).[26] The purified dextran-containing vesicles were incubated under different conditions and the leakage of the dextran was determined over time by iterative SEC to separate the dextran containing vesicles from the leaked dextran (Figures S32-S38). Similar to previous studies, here the extent of leakage of dextran 10 kDa, which is a large hydrophilic molecule, is used to provide an idea about structural stability of the vesicle membrane that is not apparent by the mere observation of large MLVs, MVVs and ULVs by fluorescence spectroscopy.[26,59] The 2:1 DA:cPC10 was found to retain about 80% dye over 48 hours while the 5:1 GMD:cPC10 exhibited higher retention capacity of 95% over 48 hours (Figures S32, S35).

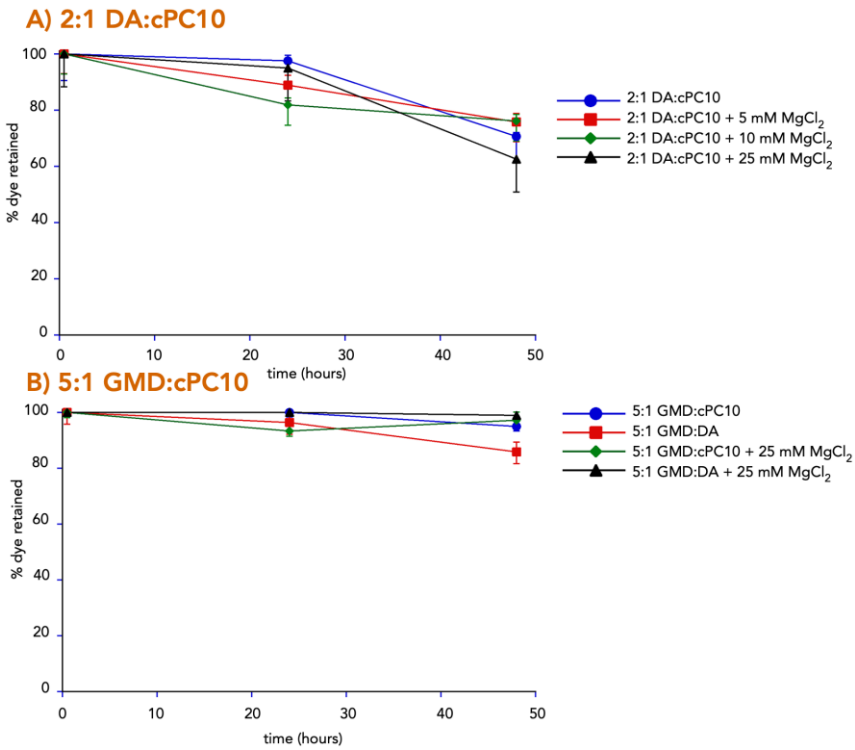

Figure 6. Comparison of the stability of vesicles from 2:1 DA:cPC10 versus 5:1 GMD:cPC10 system in the presence of Mg^{2+} as monitored by dye leakage over time. Retention of fluorescently (AF-488) labeled dextran 10 kDa in cPC10-based vesicles (total concentration 40 mM) over a period of 48 h of (A) 2:1 DA:cPC10, pH 6.6; (B) 5:1 GMD:cPC10, pH 6.3. Lines connecting the data points are visual guides only. Error bars are ±SD. For more information see SI (Figure S32-S38).

The increased stability of GMD:cPC10 system due to the inclusion of GMD is in consonance with what is known in DA-based vesicles.[30] The 2:1 DA:GMD system showed similar propensity (80% retainment, Figure S34B) as 2:1 DA:cPC10 while the corresponding 5:1 GMD:DA system under the same conditions retained about >85% (Figure S36) comparable to the 5:1 GMD:cPC10 system's >95%. Similar comparison of the 2:1 DA:cPC10 system with vesicles derived from the corresponding pure DA system under identical conditions (40 mM, pH 6.6) was not possible since DA-system with AF488-dextran 10 kDa were found to be unstable to the SEC purification procedure, a behavior that has been reported previously[60]. Thus, the inclusion of cPC10 into vesicles seems to offer better membrane stability when compared to DA, as noted before with cPC10:dodecanol versus corresponding DA-based systems.[26]

Based on the effect of Mg^{2+} on the stability of these two cPC10 containing vesicle systems we studied the leakage of the dye in the presence of 25 mM of Mg^{2+}. In the case of 5:1 GMD:cPC10 we observed > 95% retention over 48 hours (Figure S37). For the 2:1 DA:cPC10 system we tested up to 10 mM of Mg^{2+} and observed about 80-90% retention at 48 hours (Figure S34A). However, we did observe some flocculation with 10 mM Mg^{2+} after SEC isolation of vesicles containing the dye at 24 hours (Figure S33). The parent system 5:1 GMD:DA system was also stable and was found to retain ~ 99% of the dye over a period of 48 hours even in the presence of 25 mM Mg^{2+} (Figure S38).

The overall observations suggest that this cPC10 containing heterogenous system is quite dynamic and can be influenced by a variety of factors such as pH, temperature and metal ions. Furthermore, our results thus far also indicate that cPC containing vesicles (especially with GMD) are resilient and encode the ability to recover from destabilizing fluctuations in environmental conditions such as excursions to higher metal ion concentrations, temperatures or extrusion through small pores, all of which could have been relevant in plausible prebiotic scenarios.

Some of the morphological changes and growth behavior could be related to the mechanism that has been postulated for the oleate derived vesicles where the addition of di-oleyl phosphatidic acid (DOPA) led to protocell membrane growth.[16] Further physical studies are ongoing in order to understand the mechanisms behind the growth and morphological

transformations in these cPC10-based systems and how (and if) they differ from the fatty acid-based systems.

Glyceryl didecanoate phospholipids GDDP1 and GDDP2 based systems also form vesicles but with important differences when compared to the cPC10-based systems: The 1,2-didecanoate GDDP1, **10a** and 1,3-didecanoate GDDP2, **10b** have (a) two C10-acyl chains and (b) a phosphate moiety instead of a phosphodiester group. Thus, the vesicles formed from GDDP1- and GDDP2-based systems, not unexpectedly, showed divergent behavior and properties when compared with the phosphodiester cPC10-based systems. We synthesized GDDP1 and GDDP2 by adapting literature procedures (see SI for details).

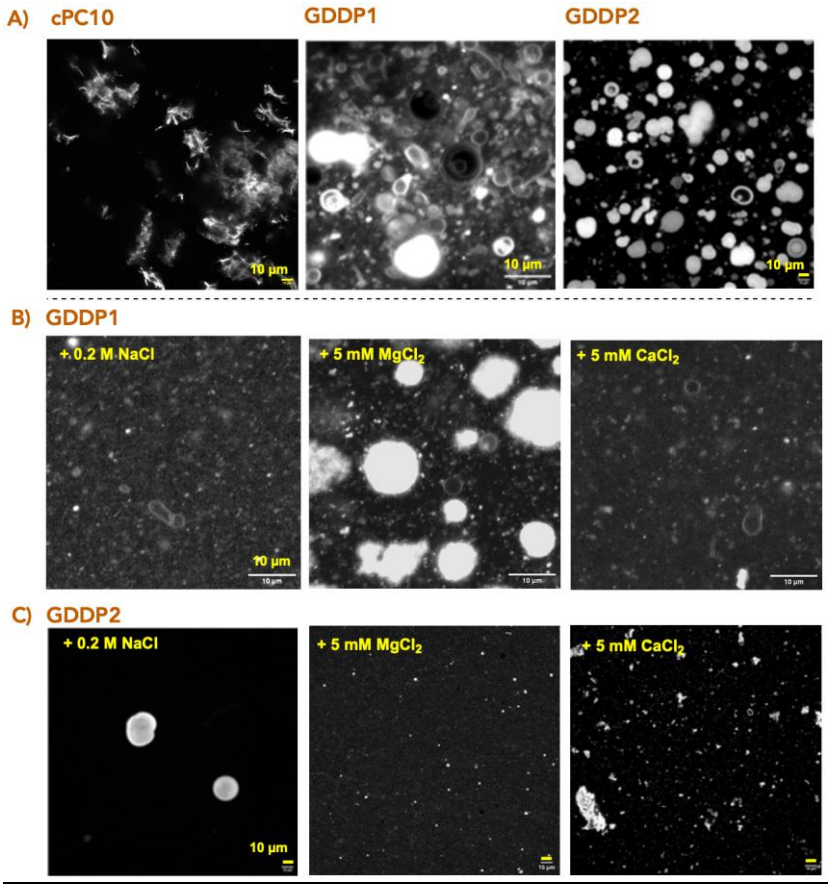

Figure 7. GDDP1 and GDDP2 by themselves form vesicles (unlike cPC10) but are more susceptible to the presence of metal ions in comparison to cPC10-based vesicles. Confocal microscopy images (A) comparing the vesicle forming propensity of cPC10 (20 mM, pH 6.6), GDDP1 (20 mM, pH 6.3) and GDDP2 (10 mM, pH 6.6) measured at 24 h; (B) and (C) comparing the effect of metal ions on the vesicles in the GDDP1 and GDDP2 (at 24 h). Vesicles are labeled with R6G. Scale bars represent 10 µm. For more information see SI (Figure S39, S42-44 for GDDP1, Figure S50, S53, S56 for GDDP2).

Monophosphate double-chain GDDP1 **10a** and GDDP2 **10b** by themselves form vesicles which are stable under a narrow range of conditions: We observed that GDDP **10a** and **10b** by themselves were capable of forming vesicles under conditions where cPC10 by itself did not (Figure 7A). The CAC for both GDDP systems was around 1.5 mM as opposed to the 10 mM reported[26] for cPC10. Strikingly, although the total concentration of acyl chains for the GDDP systems is twice that of the same molecular concentration of cPC10, the CAC is lower by a factor of around 7. This could be a result of increased hydrophobicity and a polyvalency effect due to the second linked C10-acyl chain in the GDDP systems. GDDP1, **10a**[15] generally formed more ULVs and thin-walled MVVs and MLVs as opposed to GDDP2 **10b** which formed thick-walled MLVs (Figure S39-S41 versus Fig S50-S52). The optimal pH range was 6.0-6.6; increasing the pH to 7.0 and beyond led to decreased propensity or absence of vesicles in both systems (Figure S41 & S50-51). This behavior can be understood based on the extra negative charge on the phosphate (as opposed to the single negative charge on the cPC10) and higher second pKa of the phosphate (≈ 7) when compared to that of cPC10 (≈ 2) – which

causes the GDDP-based systems to change their protonated-deprotonated status depending on the pH ranges of 4.0-8.5, leading to repulsion at higher pHs.[19] In a 0.2 M phosphate buffer (pH ≈ 6.5), GDDP1 vesicles were stable while the GDDP2 system did not form vesicles (Figure S47 versus S59), but did so in a 0.05 M phosphate buffer (Figure S47, S59). Together, these results can be rationalized based on a combination of charge, hydrophobicity and polyvalency effects, with additional differences emerging between the GDDP1 and GDDP2 isomers.

The presence of a phosphate-moiety in GDDP also caused the pure GDDP-based vesicles to be more sensitive to presence of metal ions at lower concentrations when compared to phosphodiester cPC10-based systems (Figure 7B-C). For example, concentrations of Na^+ (up to 0.2 M) and Mg^{2+} (5-10 mM) were barely tolerated for vesicles from GDDP1 **10a**, while higher concentrations of metal ions led to precipitation and flocculation (Figures S42-S45). The GDDP2-vesicles from **10b** while stable to 0.2 M Na^+ (Figures S53-55), were precipitated/flocculated even with 5 mM of Ca^{2+} or 10 mM Mg^{2+} (Figure S56). Thus, the presence of short didecanoate-chains seems not to overcome the deleterious effect of divalent metal ions indicating that the number of phosphate charges exerts greater control at the C10 short-chain fatty acid stage of phospholipids.[15,48]

GMD:GDDP1 and GMD:GDDP2 systems form stable and robust ULVs and MLVs respectively over a range of ratios, pH and metal ion concentrations: As was observed with the cPC10-based vesicles, addition of GMD **7** to GDDP **10a** or **10b** at various ratios led to more robust vesicles (with respect to pH and metal ions) when compared to the pure GDDP-based vesicles (Figures S39-S45 and S50-S58). Interestingly, the CAC for the GMD:GDDP systems (Table S3, S4) was around 1.5 mM (similar to that of the GMD:cPC10 and the pure GDDP systems) and did not vary with the increasing amount of GMD, which may reflect a balancing of stabilizing (lowering charge repulsion/H-bonding) and destabilizing (single acyl chain) effects of GMD vs GDDP. Based on the variation of ratios and pH we chose the 5:1, 2:1, 1:1 in the GMD:GDDP systems to investigate their behavior with respect to the effects of pH, metal ions and their ability to retain AF488-dextran 10 kDa with time.

Inclusion of GMD with GDDP provides vesicles with a tangible tolerance to pH and metal ions, with GMD:GDDP1 combination being more robust than GMD:GDDP2 (Figure 8): The presence of GMD enabled the GDDP-based vesicles to form at higher pHs 7.0-8.5 (Figures S41, S50-51) pointing to the mitigating effect of the hydrogen-bonding with the hydroxyl groups of GMD even with the increasing negative charges on the phosphate. The GMD:GDDP1 based compositions formed giant vesicles in phosphate buffer concentrations of 0.05-0.2 M buffer (Figure S47), while the GMD:GDDP2 based vesicles formed at 0.05 M and not very well at 0.2 M phosphate buffers (Figure S59). At lower pH of 4.0 and 5.0 the GMD:GDDP1 based systems (Figure S41) showed dynamic behavior where (a) inner protrusions of an MLV starting from one side reaches over and fuses on the opposite side to produce a "trans-membrane vesicle" (Video S14) and (b) in MVV the smaller vesicles inside the larger vesicle fused with the membrane of the larger vesicle (videos S16-S27). The GMD:GDDP2 vesicles formed over a wide range of ratios (1:2 to 9:1), pH (4.0-8.5), and concentrations (40-2.5 mM) and were stable over days (Figures S50-52, videos S28-S30). As expected from the pKa values, increasing the ratio of GMD:GDDP2 to 1:5 led to vesicle formation only when the pH was lower than 7.0; above pH 7.0 it formed oil droplets (Figures S50-S51). GMD's presence in the GDDP series improved the tolerance to metal ions with the 5:1 GMD:GDDP1-system faring the best enduring concentrations up to 0.4 M of Na^+, or 25 mM Mg^{2+} or Ca^{2+} ions (Figures S42-S44); at the higher end of Mg^{2+} ions,

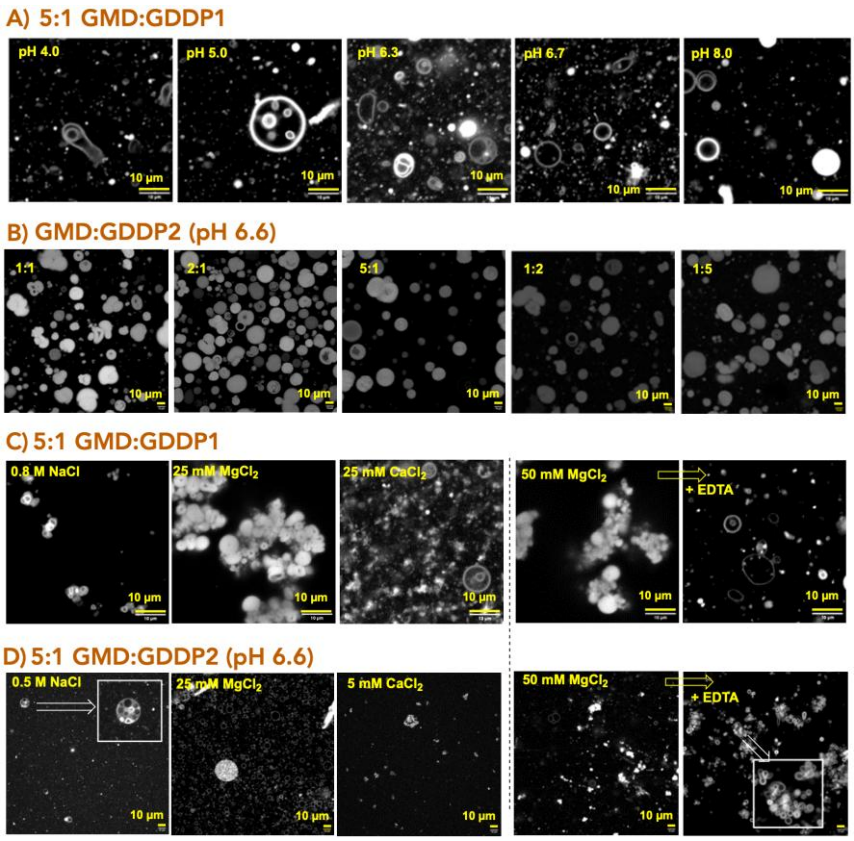

Figure 8. GMD:GDDP vesicles are more stable over a wide range of pH, composition with increased tolerance to metal ions. Confocal microscopy images showing (A) the range of pH over which the 5:1 GMD:GDDP1 (total concentration 20 mM) vesicles are formed (measured after 24h); (B) the vesicles forming from various ratios of GMD:GDDP2 at pH 6.6 (after 24 h). (C) Effect of metal ions on the 5:1 GMD:GDDP1 at pH 6.3 (after 24 h) and recovery of vesicles from 5:1 GMD:GDDP1 In the presence of 50 mM of Mg^{2+} with 50 mM of EDTA, and (D) Effect of metal ions on the 5:1 GMD:GDDP2 at pH 6.6 (after 24 h) and recovery of vesicles from 5:1 GMD:GDDP2 in the presence of 50 mM of Mg^{2+} with 50 mM of EDTA. Vesicles are labeled with R6G. Scale bars represent 10 µm. For more information see SI (Figure S41-S46 for 5:1 GMD:GDDP1; Figure S50, S53, S56, S57 for 5:1 GMD:GDDP2).

the 5:1 GMD:GDDP1 vesicles started to morph into thick multilamellar shapes, while Ca^{2+} ions seemed to form unilamellar structures with increasing flocculation over time (Figure S43).[48] In the case of 5:1 GMD:GDDP2, higher Mg^{2+} ion concentrations over time led to fluidic structures which resembled the behavior of pure GMD with the salts (Figures S53, S55-S56) – suggesting that GDDP2 was being removed from the system leaving the GMD in solution. Moreover, the presence of 0.2 M NaCl was not able to mitigate the flocculation in the presence of Mg^{2+} (unlike the cPC10-based systems[26]). Using synthetic sea-salt in place of the individual metal ions resulted in flocculation behavior (Figure S56) at concentrations that were consistent with the above observations with GMD:GDDP1 systems giving rise to remodeling of vesicles at higher synthetic sea salt concentrations. The GMD:GDDP1 system tolerated higher amounts of sea salt when compared to the GMD:GDDP2 system (Table S5) consistent with the observations above. In an effort to understand whether the precipitation and flocculation of the vesicles from the GMD:GDDP caused by divalent metal ions can be reversed, we added EDTA to the 5:1 GMD:GDDP systems that have been flocculated or precipitated in the presence of 25 mM Mg^{2+}. And observed that -with time- the system reformed ULVs in the 5:1 GMD:GDDP1 series (Figure S46) and the MLVs in the 5:1 GMD:GDDP2 series (Figure S57, Video S31-S32). A control experiment of EDTA addition to the GMD:GDDP systems showed that the presence of EDTA does not have a substantial effect on the vesicles (Figure S46, S57) – thus suggesting it is the sequestering of the divalent metal ions by EDTA that is responsible for reversing the effect caused by the metal ions.[15,48]

Vesicles from the pure GDDP and the hybrid GMD:GDDP series retain AF488-dextran 10 kDa dyes: We probed the integrity of the vesicles in this series with AF488-dextran 10 kDa dye and observed that both the pure GDDP and the GMD:GDDP series (5:1 in the case of

GDDP1 and 2:1 and 5:1 for GMD:GDDP2) retained the dextran quite well over 48 hours (Figures S61-S65). The pure GDDP vesicles retained ≈95% of the dextran in 48 hours. In the presence of Na^+ (in the ranges from 0.2 M – 0.7 M) the 5:1 GMD:GDDP1 vesicle retained about 90-64% of the dextran while in the case of 2:1 to 5:1 GMD:GDDP2 up to 0.2 M NaCl showed >90% retainment over 48 h (Figure 9).

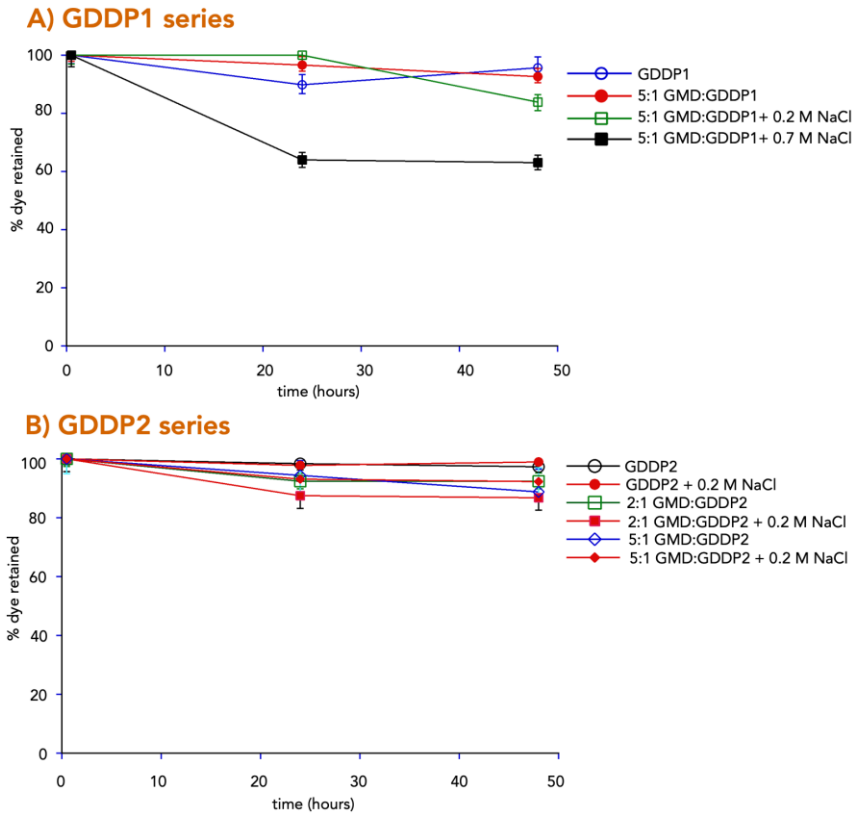

Figure 9. Comparison of the stability of vesicles from the pure GDDP systems versus 5:1 GMD:GDDP systems in the presence of Na^+ as monitored by dye leakage over time. Retention of AF-488 labeled dextran 10 kDa in GDDP-based vesicles over a period of 48 h of (A) GDDP1-based system as a function of Na^+ ion concentration at pH 6.3; (B) GDDP2-based system as a function of Na^+ ion concentration at pH 6.5. Lines connecting the data points are visual guides only. Error bars are ±SD. For more information see SI (Figure S61-S65).

This behavior is better than the corresponding cPC10 based tertiary systems reported before[26] and similar to the GMD:cPC10 systems shown above. We could not investigate the effect of divalent metal ions on the retention of AF488-dextran 10 kDa in the GDDP series since precipitation over time interfered with size exclusion chromatography step that was necessary to purify the vesicles containing the dextran from the free unencapsulated dextran.

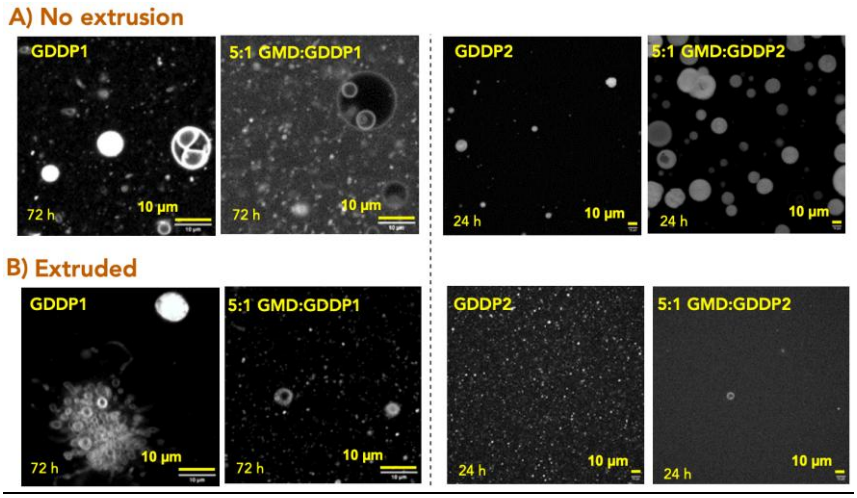

Figure 10. GDDP1-based vesicles show more ULVs compared to GDDP2-based vesicles before and after extrusion. Confocal microscopy images of the (A) unextruded vesicles (B) extruded vesicles (0.4 µm polycarbonate membrane) from GDDP1 and 5:1 GMD:GDDP1, pH 6.3 (72 h) and GDDP2 and 5:1 GMD:GDDP2 at pH 6.5 (after 24 h). The samples were labeled with R6G. The scale bars represent 10 µm. For more information see SI (Figure S48 for GDDP1, 5:1 GMD:GDDP1; Figure S50, S55 for GDDP2, 5:1 GMD:GDDP2).

Vesicles from the pure GDDP and the hybrid GMD:GDDP series exhibit different behavior after extrusion (Figure 10): Upon extrusion (11 times) through a 0.4 micron membrane, vesicles from the pure GDDP series grew back to 5-10 micron sizes over 48-72 h period, with GDDP1 exhibiting more ULVs (Figure S48) while GDDP2 gave thick-membraned MLVs (Figures S50-S51). When the vesicles in the 1:1, 2:1 and 5:1 GMD:GDDP1 series was extruded via 0.4 micron membrane (11 times) and allowed to equilibrate, over time (72 hours) giant vesicles, 1-10 micron sizes, were reformed (Figure S48). While this is similar to the behavior of the cPC10 containing vesicles, the number of giant vesicles in the GDDP1 series were less in number compared to cPC10 series. In the case of GDDP2 and its corresponding GMD 1:1, 2:1 and 5:1 mixtures, the extrusion process led over time to dense population of vesicles with sizes less than 1 micron with few vesicles around the 2-10 micron sizes (Figure S50-S51). The extruded vesicles in the GMD:GDDP series seemed to be more affected by divalent metal ion concentrations (Figures S44, S45, S53, S55) when compared to the non-extruded samples, with the 5:1 GMD:GDDP systems once again faring better than the others. This may be related to the presence of more ULVs (which are generally less stable) in the extruded samples versus the MVVs and MLVs (more stable) in the non-extruded samples.[28]

Overall, the GDDP1 based systems tolerated pH ranges, phosphate and divalent metal ions better than the GDDP2 based systems. Both of them also formed diverse morphological structures with dynamic behavior of fusion and division (videos S16-S30). The difference in behavior of the GDDP1, **10a**- versus GDDP2, **10b**-based vesicles with respect to stability to pH, phosphate buffers, metal ions and morphological changes after extrusion, suggests that they must be related to how the phosphate and the didecanoate chains in **10a** versus **10b** are self-assembled and positioned in their respective supramolecular assemblies. And can be correlated to the 1,3-symmetric structure in GDDP2 versus the 1,2-asymmetric structure in GDDP1, in turn affecting the curvature/other properties of the membranes and, subsequently their interaction with the divalent metal ions. Such a difference is reminiscent of the contrast in the physicochemical properties of 1,2-sn-diacylglycerol versus 1,3-sn-diacylglycerol and how they pack differently in crystalline arrangements – which is suggestive of how they may affect the structure and curvature differently when incorporated into membranous structures.[61,62] Whether such differences even at the C10-level are of significance and can lead to an evolutionary selection between the symmetric (**10b**) versus asymmetric (**10a**) arrangement of phospholipids, resulting in the predominance of the asymmetric phospholipids in extant cells[63,64] needs further investigation.

Effect of addition of choline chloride or ethanolamine on the vesicles from pure GDDP (Figure 11): Since the vesicles were formed from GDDP1 or GDDP2 alone (unlike cPC10) but were more sensitive to the presence of the positively-charged metal ions (when compared to cPC10) – we wondered what the effect of the addition of positive charges in form of choline would be. The choice of choline was dictated by their plausible prebiotic availability and by the use of this amino-ethanol based moieties in extant phospholipids.[14,65-68] We also used

ethanolamine as another candidate which also served as a control to compare with choline. Therefore, we titrated in various equivalents of choline chloride and ethanolamine to the vesicles formed from only GDDP1, **10a** and GDDP2, **10b** and observed that increasing their amount led to interesting clustering and morphological changes (Figure 11).

In the GDDP1 series, the vesicles changed from ULVs to MLVs and MVVs by the addition of choline chloride or ethanolamine, however there was a difference in the type of lamellarity of the MLVs formed between the two additives (Fig S49). The vesicles from ethanolamine addition to GDDP1, **10a** gave rise to much thicker walled MLVs. When the GDDP1-vesicles were extruded to form ULVs and then exposed to choline chloride or ethanolamine, the presence of choline chloride led to thicker lamellar MVVs while the addition of ethanol amine led to more GUVs (Figure S49). In the case of the GDDP2, the addition of choline chloride led to a remarkable change to MVVs that resemble a collection of many MLVs and ULVs within a giant vesicle of 10-20 μm diameter in 24 hours (Figure S60). With time, the vesicles settled around 2-5 μm which was similar to the sizes from the control (no choline chloride addition), but still retained the MLV and MVV character. Furthermore, the extruded GDDP2-vesicles in the presence of choline chloride formed a large (10-15 μM) collection of 'clusters' of ULVs (Figure S60, Video S33- S35). The addition of ethanolamine, on the other hand, led to persistence of the MVVs and MLVs with time (Figure S60).

Overall, the addition of choline or ethanolamine produces vesicles that are largely similar in nature (lamellarity, shape and size) to those obtained from the GMD:GDDP hybrid systems. The results from the addition of choline and ethanolamine suggests that the beneficial non-covalent effects of these cationic additives could be made more 'durable' by forming a covalent bond between these additives with the phosphate group of GDDP – as observed in extant lipid structures.

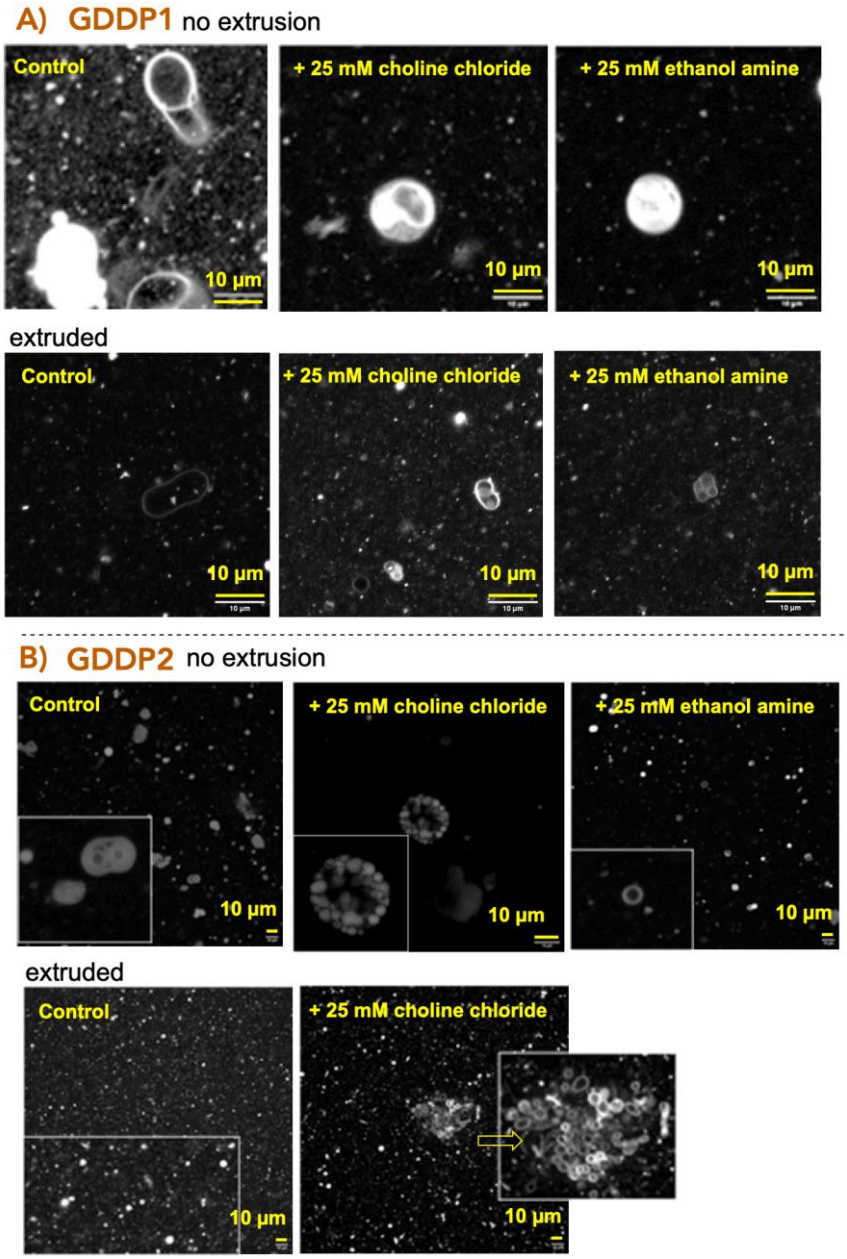

Figure 11. Pure GDDP vesicles show different morphological behavior in the presence of choline and ethanol amine. Confocal microscopy images of the (A) vesicles from GDDP1 and (B) from GDDP2, in the absence (control) and presence of choline chloride (25 mM) and ethanol amine (25 mM) at 24 h for extruded (through 0.4 µm polycarbonate membrane) and unextruded samples. The samples were labeled with R6G. The scale bars represent 10 µm. For more information see SI (Figure S49 for GDDP1; Figure S60 for GDDP2).

The added benefit of forming a phosphodiester derivative (from GDDP) would result in reduced negative charges on the phosphate (from two to one) by converting it to a choline-phosphodiester and perhaps leading to more robust vesicles even at C10-level that can withstand variations of prebiotic conditions. Such a study -which is beyond the scope of this paper- is underway in our lab and will be reported in due course. In this context, it is notable that Bonfio and co-workers[69] have shown a plausible prebiotic route to diverse ethanol amine phospholipid headgroups that provides support for the hypothetical scenarios discussed in our work.

Crude reaction mixtures generated from plausible prebiotic reaction contain cPC10, GMDP1, GMDP2, GDDP1 and GDDP2, and also form vesicles.

With the above demonstrations of clean mixtures generated from pure synthetic compounds **8**, **9a**-**10b**, we investigated whether a messy mixture resulting from a plausible prebiotic reaction scenario would also generate these phospholipids and lead to emergence of vesicles in the same scenario (Figure 12). Based on our previous work[25] we turned to the DAP mediated concomitant esterification and phosphorylation of glycerol in the presence of decanoic acid. As an additional path we also studied whether the hydrolysis of the cPC10 followed by DAP-mediated esterification reactions with decanoic acid would lead to the GDDP-types of molecules proposed in Figure 1. First, we hydrolyzed cPC10, **8** to the corresponding GMDP (1- and 2-phosphates) **9a** (GMDP1, glyceryl 3-monodecanoate 1-phosphate) and **9b** (GMDP2, glyceryl 1-monodecanoate 2-phosphate) based on previous procedure.[27] The hydrolytic opening of the cyclic phosphate group of cPC10 is slow (on the order of days-weeks at pH 4). Therefore, we employed a lower pH of 2-3 for the sake of expediency. This resulting crude mixture of **9a** and **9b** was subjected to wet-dry cycles in the presence of moist-paste of DAP and decanoic acid in the presence and absence of Mg^{2+}. LC-MS analysis of this mixture in both cases showed the formation of GDDP (ascribable to **10a**/**10b**) as constituents along with cPC10, **8** and starting GMDP **9a** and **9b** (Figure S66). These crude reaction mixtures were used to prepare vesicles (using the same procedure for the cPC10 and GDDP series), we observed giant 5-20 μm unilamellar and oligolamellar vesicles at pH 6.6 using R6G dye (which was reproducible, Figures S67, S68). We also were able to observe entrapment of AF488-labeled dextran 10 kDa within the lumen of these structures, thus confirming the formation of vesicles (Figure 12A, Figure S67).

We then took a step back and subjected a moist-paste mixture of decanoic acid and glycerol alone in the presence of DAP and imidazole to the wet-dry cycles to see if these higher order products (as proposed in Figure 1) would still be produced. When the reaction mixtures (with and without imidazole) were analyzed by LC-MS (Figure S69), we observed once again the formation of GMDP **9a**/**9b** and GDDP **10a**/**10b** (among other species) in the reaction mixture that contained imidazole (Figure 12B). In the mixture without imidazole, GMDP **9a** and **9b** were identified. And when these crude reaction mixtures were mixed with a pH 6.6 buffer, the mixture that contained the GDDP **10a**/**10b**, generated in the presence of imidazole, showed more robust vesicle formation (MLVs and MVVs) compared to the one in the absence of imidazole which showed formation of GMDP **9a** and **9b** (Figure S70). Thus, these results from the prebiotic reaction mixture provides support for the early emergence of phospholipids and, in combination with the above studies, also for their role in the emergence of protocells.

DISCUSSION

The above studies highlight one possible pathway for how phospholipids can emerge as part of the primeval chemical evolutionary process, when phosphorylation step is introduced as early part of the prebiotic chemical scenario.[14] Our study has focused on the early role of cyclic-phospholipids (e.g., cPC10) in such a scenario based on (a) its formation under plausible prebiotic conditions from the same type of prebiotic building blocks of short chain fatty acids and glycerol[25] and (b) its ability to form vesicles and protocells as a ternary mixture with prebiotic components such as short chain fatty alcohols and GMD[26]. We show that simpler binary mixtures –resulting from cPC10 **8** with its own precursor building blocks

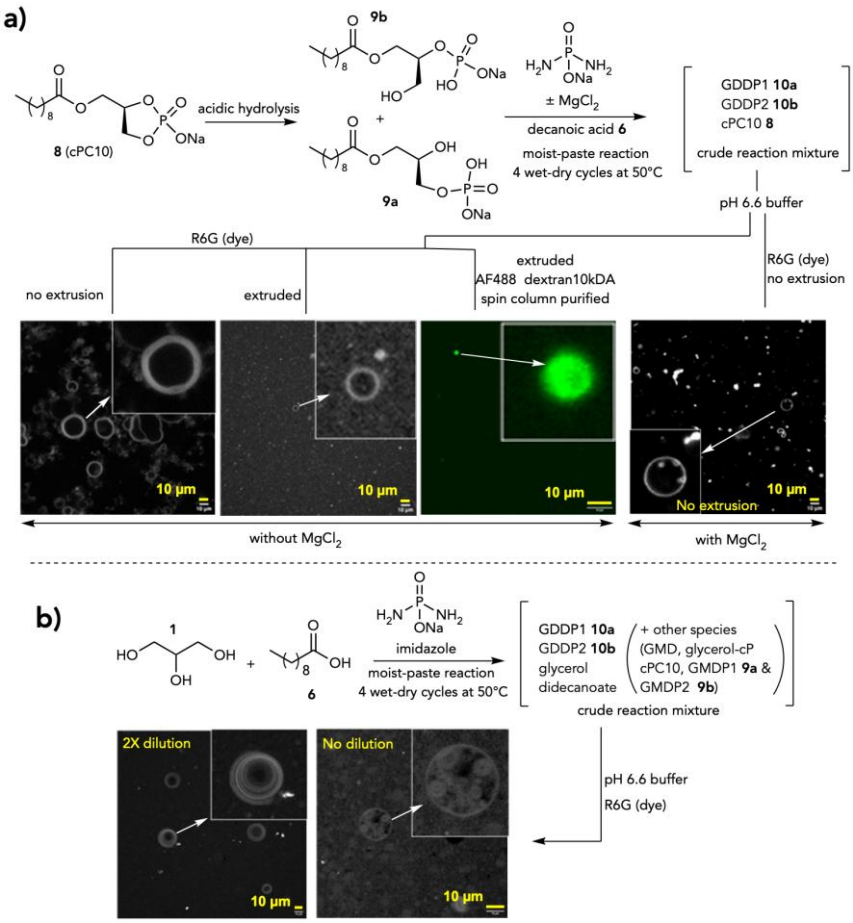

Figure 12. Mixtures of phospholipids formed by plausible prebiotic reaction produce vesicles consistent with those derived from the pure components. Confocal microscopy images of the crude mixtures produced from (A) the hydrolysis of cP10 **8** and the reaction of the resulting products (GMDP1 (**9a**) and GMDP2 (**9b**) with DAP and decanoic acid with/without Mg^{2+}. Confocal images of the crude reaction mixture (after 4 cycles), labeled with R6G or AF488-dextran 10 kDa at pH 6.6, 50 °C (measured after 24 h equilibration). (B) The reaction of decanoic acid and glycerol with DAP, under the moist-paste wet-dry cycle reaction conditions at 50 °C. Confocal images of the crude reaction mixture (after 4 cycles), labeled with R6G at pH 6.6, 50 °C (measured after 24 h equilibration). The scale bars represent 10 µm. The sample labeled with AF488-dextran 10 kDa dye was purified through spin-column and measured. For more details see SI (Figure S66-S70).

decanoic acid (DA) **6** and GMD, **7**– themselves can give rise to a wide spectrum of vesicles with varied properties. The cyclic phosphate moiety represents the simplest form of phosphodiester containing one negative charge and mimics the phosphodiester nature of modern phospholipids with significant differences – in the shape of the head group, due to the cyclic phosphate in the cPC (as opposed to the linear phosphodiester) and having one long acyl chain (instead of two). Thus, while the DA:cPC10 based systems form a variety (ULV, MLV, OLV and MVV) of vesicles depending on the pH, the GMD:cPC10 mixtures gives rise to an assortment of MLVs spanning a wide pH (5-8) range. The formation of multilamellar- and oligolamellar- and multi-vesicular vesicles have been noted to offer advantages over ULVs, since they are less prone to rupture and leakages under stress.[28] And their formation seems to explain the stability of many of these cPC10-based vesicles to high concentrations of divalent metal ions such as Mg^{2+} and Ca^{2+} and the extrusion processes. The morphing of some of these vesicles with change in pH and presence of divalent metal ions presents further opportunities to exploit them for growth and/or division by a simple change of environmental conditions.[44]

Moreover, the same cyclic phosphate moiety allows for further reaction with nucleophiles to give higher order phosphodiesters or hydrolytic opening to form the mono-phosphate fatty acids esters **9a** and **9b**, enabling further progression from the monoacyl-cPC10 towards the next level of diacyl-phospholipids GDDP1 **10a** and GDDP2 **10b**. Though it is possible that the mixtures of GMD with **9a** or **9b** could also give rise to vesicles, we have not investigated this scenario in this study – due to our interest in investigating the diacyl-phospholipid derivatives. These diacyl-phospholipids by virtue of having two fatty acid chains have lower CAC, allowing for vesicles to form at much lower concentrations compared to cPC10-based systems. Consequently, the GDDP either by themselves or as admixtures with GMD, exhibit properties different from the cPC10-based vesicles. While the gains (over mono-acyl cPC10) due to the diacyl-moiety in GDDP are compromised to some extent by the presence of the phosphate (two negative charges) in GDDP that increases the sensitivity to divalent metal ions, this shortcoming could be overcome by the addition of GMD. Furthermore, there seems to be differences emerging between the vesicles based on GDDP1 versus those composed of GDDP2 on how they respond to a variety of conditions. Whether such differences (manifested at a C10 level) can be extrapolated to longer phospholipid sequences and explain the coincidental presence of the sn-1,2-asymmetric GDDP1 type structures in cell membranes in extant biology is unclear, necessitating more in-depth investigations.

Thus, the range of vesicle morphologies stemming from the progression of cPC10 to GDDP based systems offer a variety of properties in terms of ease of formation, stability with respect to pH, variations of temperature and metal ions. Such a concatenation of constitutionally related vesicles and their emerging properties offer a multitude of candidate-vesicles for further studies at many levels[70] such as (a) dynamic shapes lending themselves to growth and division, (b) replication of nucleic acids that rely on divalent metal ions dependent activation chemistries, and (c) hosting network of protometabolic reactions, to name a few. It is quite possible that a particular constituent-vesicle may be better suited for oligonucleotides replication studies while another kind of vesicle may be suited better for hosting protometabolic reactions or growth and division. Therefore, while it may be natural to search for one particular vesicle-system as “a solution” for a particular scenario, it may not be optimal at the prebiotic level in the long run. Rather it may be prudent to explore the “vesicle-library space” of a range of related compositions to see what opportunities naturally emerge.[4] It may turn out the apparently differing optimal systems generated within a given composition can interact (“mix”) over time, and newer systems and unanticipated properties may emerge. One such intriguing possibility is whether the protocells themselves may act as ‘catalysts’ for certain reactions, a possibility that has been discussed in the context of a lipid-based model.[71] And this could add another dimension of augmenting processes that feedback into the systems chemistry co-evolutionary scenario.

Moreover, the presence of prebiotically plausible organic molecules could add another level of selection, and those non-covalent effects are not easily foreseen as part of chemical evolutionary scenario. It is for these reasons our investigation was designed to be agnostic with respect to the mapping of the landscape of vesicles stemming from the cPC10-based systems and not driven by trying to find “the optimal” protocell with one reaction scenario in mind. Whether the cPC10- and GDDP-based vesicles are useful in terms of hosting reactions of prebiotic interest (such as oligonucleotide replication demonstrated in other fatty acid based systems)[28,72] remains to be demonstrated and ongoing work in other laboratories[70] may shed light on these possibilities. And the next logical challenge would be if those ‘internal’ processes could be coupled to the dynamic behavior of the phospholipid vesicles (as seen in the videos S1-S35) for growth and division.

In the context of the effect of the presence of organic molecules, the addition of choline and ethanol amine and their non-covalent effect was considered in our work based on the hypothesis that these positively charged amine systems would affect the GDDP-based vesicles and may help to minimize the shortcomings of the effect of monophosphate (two negative charges) on the supramolecular assemblies. The preliminary results seem to indicate that there is remodeling of the GDDP-vesicles in terms of the shapes and morphology based on these non-covalent charge-based interactions. This suggests that if these interactions could be made ‘permanent’ by a covalent linkage (via the formation of a choline- or ethanol amine-link)[69] to the phosphate group, it would not only reduce the two negative charges in the GDDP to one, but also put a positive charge closer to the resulting

phosphodiester bond that will mitigate any deleterious repulsion that can result in the absence of hydrogen-bond mediated associations and compromise vesicle integrity. Thus, it is clear that addition of small molecules capable of non-covalent interactions may also play role in the chemical evolution of phospholipids. In that context, it is important to note that we have not considered the effects of other prebiotically relevant compounds such as amino acids/peptides and nucleic acids. Such studies have been reported on fatty acid vesicles[8,73,74] and it would be the next natural step to extend these types of experiments to the phospholipid systems described in our work.

In addition to the cPC-phospholipid scenario described above, introducing the phosphorylation at the very early stage of chemical evolution may give rise to other chemical evolutionary pathways. For example, we have observed in our previous work the formation of cyclic phosphate of glycerol as a discrete intermediate on the path towards cPC-phospholipids.[25] Thus, there could be other pathways, such as the reactions of cyclic phosphate of glycerol directly with nucleophiles to give rise to the GDDP-type molecules or acylation of glycerol phosphates, pathways that have been considered and investigated by others as well.[14,15,69]

Thus, our observations coupled with the works of others suggest that transformation from the primordial vesicles to functioning protocells can be probed via studying a spectrum of dynamically varying vesicles' compositions and, therefore, their evolving and emerging properties. Importantly, it suggests that the emergence of phospholipid-based vesicles can be early in the series of prebiotic events, concurrent with those based on fatty acids in a systems chemistry context – rather than as a separate, discrete and later evolutionary development. While the idea of early phospholipids-based protocells is in consonance with recent reports,[14,15,69] there has also been arguments for heterogeneity in lipid composition as a necessary (intermediate) part of transition from vesicles based on fatty acids to those composed of phospholipids.[10,50] Our results bring attention to another possibility that –from the very beginning– there may be a continuous spectrum of hybrid-composomes[75] of vesicles with varied amalgam of the starting materials, intermediates and products. Such a systems chemistry in protocell evolution would be compatible with other systems chemistry perspectives in prebiotic chemistry and chemical evolution.[4,76]

EXPERIMENTAL PROCEDURES

Resource availability

Lead contacts

Further information and requests for resources should be directed to and will be fulfilled by the lead contact, Ramanarayanan Krishnamurthy (rkrishna@scripps.edu).

Materials availability

All materials generated in this study are available from the lead contacts without restriction.

Data and code availability

This study did not generate any datasets.

SUPPLEMENTAL INFORMATION

Document S1. Supplemental experimental procedures, Figures S1–S86, Table S1-S5, Schemes S1-S4 and NMR spectra.

Video S1. Part 1 of movie showing the effect of heating on 2:1 DA:CPC10 mixture. 40 mM of the 2:1 DA:cPC10, labelled with R6G (0.01 mM) heated to 60 °C. Frame interval: 1.0 sec.

Video S2. Part 2 of movie showing the effect of cooling on 2:1 DA:CPC10 mixture and its transformation. 40 mM of the 2:1 DA:cPC10, labelled with R6G (0.01 mM) was heated to 60 °C and cooled where around 45 °C a dynamic change was observed with tube-like structures forming and transforming into giant uni- and multi-lamellar vesicles. Frame interval: 1.0 sec.

Video S3. Part 3 of movie showing the overall effect heating-cooling on 2:1 DA:CPC10 mixture and its transformation to vesicles. 40 mM of the 2:1 DA:cPC10, labelled with R6G (0.01 mM) was heated to 60 °C and cooled to 35 °C over a duration of 40 min resulted in a heterogenous mixture of GUVs and MLVs. Frame interval: 1.0 sec.

Video S4. Movie of MVVs formed from heating of 2:1 DA:cPC10 vesicles. 40 mM of the 2:1 DA:cPC10, labelled with AF488 dextran 10 kDa (0.02 mM) was purified by spin-column and heated to 60 °C and cooled to 35 °C (duration 40 min). Giant MVVs were observed in the videos taken at 35 °C showing that the dye has been retained inside and also incorporated in the lipid membrane. Frame interval: 0.31826 sec.

Video S5. Movie of MVVs formed from heating of 2:1 DA:cPC10 vesicles. 40 mM of the 2:1 DA:cPC10, labelled with AF488 dextran 10 kDa (0.02 mM) was purified by spin-column and heated to 60 °C and cooled to 35 °C (duration 40 min). Giant MVVs were observed in the videos taken at 35 °C showing that the dye has been retained inside and also incorporated in the lipid membrane. Frame interval: 0.15226 sec.

Video S6. Movie showing corresponding Z-stack of MVVs from Video S5. Frame interval: ScalingZ: 0.1 mm.

Video S7. Video showing a budding-type behavior of a MVV of GMD:cPC10. 40 mM of the 4:1 GMD:cPC10, in 0.2 M bis-tris buffer, pH 6.7 labelled with R6G (0.04 mM), 72 h. Frame interval: 0.78349 sec.

Video S8. Z-stack video of GMD:cPC10 vesicles. 40 mM of the 5:1 GMD:cPC10, in 0.2 M bis-tris buffer contains ~5 mM NaOH, pH 6.2 labelled with R6G (0.04 mM) taken 1 h after sample preparation. The z-stack clearly shows the 3D view of MLVs. ScalingZ: 1.99 mm.

Video S9. Movie suggestive of budding of smaller vesicle inside the giant ULV of GMD:cPC10. 40 mM of the 5:1 GMD:cPC10, in 0.2 M bis-tris buffer contains ~5 mM NaOH, pH 6.5 labelled with R6G (0.04 mM) taken 1 h after sample preparation. Frame interval: 0.78349 sec

Video S10. Movie showing the transformation to oligolamellar vesicle of GMD:cPC10. After the addition of 16. 6% of 40 mM cPC10 to 40 mM GMD at 60 °C and cooling down the sample. Movie taken at 44-43 °C. Labelled with R6G (0.02 mM) pH 6.1 in 0.2 M bis-tris buffer. Frame interval: 0.31703 sec

Video S11. Movie showing MVVs within a GUV of GMD:cPC10 vesicles. 10 mM of the 5:1 GMD:cPC10, in 0.2 M bis-tris buffer, pH 6.3 labelled with R6G (0.04 mM). Movies were captured 24 h after sample preparation. Frame interval: 0.39251 sec.

Video S12. Corresponding Z-stack of video S11 showing MVVs within a GUV of GMD:cPC10 vesicles. ScalingZ: 3 mm.

Video S13. Z-stack video showing different morphologies of GMD:cPC10 vesicles. 40 mM 5:1 GMD-cPC10 in 0.2 M bis-tris buffer pH 6.2 labelled with R6G (0.04 mM). Movies were captured within 2 h of sample preparation. ScalingZ: 3 mm.

Video S14. Z-stack video showing 3D view of vesicles from GMD:cPC10 as seen via Alexa 488 dye labelled dextran 10 kDa (inside the vesicle) and Cy5 dye (in the membrane). 40 mM 5:1 GMD-cPC10 system, pH 5.0 in 0.2 M acetate buffer, 144 h. ScalingZ: 3 mm.

Video S15. Z-stack video showing 3D view of various morphologies from GMD:cPC10 vesicles as seen via Alexa 488 dye labelled dextran 10 kDa (inside the vesicle) and Cy5 dye (in the membrane). 40 mM 5:1 GMD-cPC10 system, pH 5.0 in 0.2 M acetate buffer, 144 h. ScalingZ: 3 mm.

Video S16. Movie showing dynamic shapes of GMD:GDDP giant vesicles containing smaller vesicles. 10 mM 5:1 GMD-GDDP1 system, pH 6.3 in 0.2 M bis-tris buffer, labelled with 0.02 mM of R6G. Movies were captured 24 h after sample preparation. Frame interval: 0.24393.

Video S17. Movie showing dynamic changes of a giant MVV from GMD:GDDP. 10 mM 5:1 GMD-GDDP1 system, pH 6.3 in 0.2 M bis-tris buffer, labelled with 0.02 mM of R6G. Movies were captured 24 h after sample preparation. Frame interval: 0.24393.

Video S18. First part of a movie of GMD:GDDP vesicles showing formation of a smaller vesicle within a larger vesicle leading to oligolamellar vesicles with time. 10 mM 5:1 GMD-GDDP1 system, pH 6.3 in 0.2 M bis-tris buffer, labelled with 0.02 mM of R6G, 25 mM of EDTA was added to the sample. Movies were captured 24 h after sample preparation. Frame interval: 0.24393 sec.

Video S19. Continuation of Video S18 of GMD:GDDP vesicles showing formation of a smaller vesicle within a larger vesicle leading to oligolamellar vesicles with time. This second movie was taken within 1 min of the Video S18**.** Frame interval: 0.24393 sec.

Video S20. Movie showing the dynamics within an unusual multilamellar and multivesicular GMD:GDDP giant vesicle. 10 mM 2:1 GMD-GDDP1 system, pH 6.7 in 50 mM phosphate buffer, labelled with 0.02 mM of R6G. Movies were captured 24 h after sample preparation. Frame interval: 0.24393 sec.

Video S21. Part 1 of movie of an MVV showing the dynamics of an apparent fusion of the smaller vesicles with the membrane of the GMD:GDDP giant vesicle. 10 mM 5:1 GMD-GDDP1 system, pH 5.0 in 0.2 M acetate buffer, labelled with 0.02 mM of R6G. Movies were captured 24 h after sample preparation. Frame interval: 0.24393 sec.

Video S22. Part 2 of movie (continuation of Video S21) of an MVV showing the dynamics of an apparent fusion of the smaller vesicles with the membrane of the GMD:GDDP giant vesicle. This second movie was taken within 1 min of the first. Frame interval: 0.24393 sec.

Video S23. Movie of a GMD:GDDP giant MVV appearing to divide. 10 mM 2:1 GMD-GDDP1 system, pH 4.0 in 0.2 M acetate buffer, labelled with 0.02 mM of R6G, 144 h. Frame interval: 0.24393 sec.

Video S24. Movie showing a number of vesicles trapped within the membrane layers of a GMD:GDDP1 vesicle. 10 mM 2:1 GMD-GDDP1 system, pH 5.0 in 0.2 M acetate buffer, labelled with 0.02 mM of R6G, 144 h. Frame interval: 0.24393 sec.

Video S25. Movie showing a small vesicle trapped within the thick layers of a GMD:GDDP1 vesicle. 10 mM 2:1 GMD-GDDP1 system, pH 5.0 in 0.2 M acetate buffer, labelled with 0.02 mM of R6G, 144 h. Frame interval: 0.24393 sec.

Video S26. Movie showing an unusual trapping of MVVs within a giant oligolamellar GMD:GDDP vesicle. 20 mM 1:1 GMD-GDDP1 system, pH 6.3 in 0.2 M bis-tris buffer, labelled with 0.02 mM of R6G 10 mM of $CaCl_2$ was added after sample preparation. Movies were captured 24 h after sample preparation. Frame interval: 0.24393 sec.

Video S27. Movie showing a giant ULV hosting other ULVs in the GMD:GDDP system. 20 mM 5:1 GMD-GDDP1 system, pH 6.3 in 0.2 M bis-tris buffer, labelled with 0.02 mM of R6G, 5 mM of $MgCl_2$ was added after sample preparation. Movies were captured 72 h after sample preparation. Frame interval: 0.24393 sec.

Video S28. Movie showing giant ULV and MLV with various (tube) morphologies in the GMD:GDDP system. 10 mM of the 5:1 GMD:GDDP2, labelled with R6G (0.01 mM) at pH 6.6 in 0.2M bis-tris buffer and extruded through 0.4 mm PC membrane, 96 h. Frame interval: 1.9423 sec.

Video S29. Movies showing a giant multilamellar multivesicular vesicle from GMD:GDDP system. 10 mM of the 5:1 GMD:GDDP2, labelled with R6G (0.01 mM) at pH 6.6 in 0.2M bis-tris buffer and extruded through 0.4 mm PC membrane, 360 h. Frame interval: 0.48596 sec.

Video S30. Z-stack video of vesicles shown in video S29. ScalingZ: 0.99 mm.

Video S31. Movie showing diverse and dense vesicles formed from 5:1 GMD:GDDP in the presence of Mg^{2+} and EDTA and their dynamic behavior. 10 mM of the 5:1 GMD:GDDP2, labelled with R6G (0.01 mM) was incubated with 50 mM of $MgCl_2$ and 50 mM EDTA at pH 6.6 in 0.2M bis-tris buffer, 72 h. The movie shows the dynamic movement and pearling-like behavior of tube-like vesicles. Frame interval: 0.78502 sec.

Video S32. Movie showing another example of the dynamic behavior of diverse vesicles formed from 5:1 GMD:GDDP in the presence of Mg^{2+} and EDTA. 10 mM of the 5:1

GMD:GDDP2, labelled with R6G (0.01 mM) was incubated with 50 mM of $MgCl_2$ and 50 mM EDTA at pH 6.6 in 0.2M bis-tris buffer, 72 h. Frame interval: 0.78502 sec.

Video S33. Movie showing MLVs from 5:1 GMD:GDDP in the presence of 10 mM of choline chloride. 10 mM of the 5:1 GMD:GDDP2, labelled with R6G (0.01 mM) was incubated with 10 mM of choline chloride at pH 6.6 in 0.2M bis-tris buffer. Taken after 24 h after the sample preparation. Frame interval: 0.97 sec.

Video S34. Movie showing MVVs from 5:1 GMD:GDDP in the presence of 10 mM of choline chloride. 10 mM of the 5:1 GMD:GDDP2, labelled with R6G (0.01 mM) was incubated with 10 mM of choline chloride at pH 6.6 in 0.2M bis-tris buffer. Taken after 24 h after the sample preparation. Frame interval: 0.97 sec.

Video S35. Z-stack video of MVVs shown in Video S34. ScalingZ: 0.1 mm.

ACKNOWLEDGMENTS

We gratefully acknowledge support from the NASA Astrobiology-Exobiology grant to A.A.D. and R.K. (80NSSC20K0625) and Simons Foundation grant to R.K. (327124FY19). S.P. thanks the NASA NPP program for support. We thank Dr. Lisa Racki for the use of Molecular Devices plate reader in their laboratory and the Scripps Research Core Microscopy Facility for assistance with Confocal Microscopy measurements, and Dr. Peter Walde on constructive feedback on the manuscript.

AUTHOR CONTRIBUTIONS

R.K. conceived of the project and A.A.D. and R.K. supervised the research. S.P., K.V.S., A.A.D. and R.K. designed the experiments. S. P. and K. S. V. conducted the experiments and generated the data. M.Y. conducted preliminary experiments. R.K. wrote the paper with inputs from S.P., K.S.V., M.Y. and A.A.D.

DECLARATION OF INTERESTS

The authors declare no competing interests.

REFERENCES*

1. Deamer, D. (2017). The Role of Lipid Membranes in Life's Origin. Life (Basel) *7*, 5. 10.3390/life7010005.
2. Chen, I.A., and Walde, P. (2010). From Self-Assembled Vesicles to Protocells. Cold Spring Harbor Perspectives in Biology *2*. 10.1101/cshperspect.a002170.
3. Lopez, A., and Fiore, M. (2019). Investigating Prebiotic Protocells for A Comprehensive Understanding of the Origins of Life: A Prebiotic Systems Chemistry Perspective. Life (Basel) *9*, 49. 10.3390/life9020049.
4. Segré, D., Ben-Eli, D., Deamer, D.W., and Lancet, D. (2001). The Lipid World. Origins of life and evolution of the biosphere *31*, 119-145. 10.1023/a:1006746807104.
5. Hanczyc, M.M., and Monnard, P.A. (2017). Primordial membranes: more than simple container boundaries. Curr Opin Chem Biol *40*, 78-86. 10.1016/j.cbpa.2017.07.009.
6. Maurer, S.E., Tolbol Sorensen, K., Iqbal, Z., Nicholas, J., Quirion, K., Gioia, M., Monnard, P.A., and Hanczyc, M.M. (2018). Vesicle Self-Assembly of Monoalkyl Amphiphiles under the Effects of High Ionic Strength, Extreme pH, and High Temperature Environments. Langmuir *34*, 15560-15568. 10.1021/acs.langmuir.8b02830.
7. Maurer, S.E., Deamer, D.W., Boncella, J.M., and Monnard, P.A. (2009). Chemical Evolution of Amphiphiles: Glycerol Monoacyl Derivatives Stabilize Plausible Prebiotic Membranes. Astrobiology *9*, 979-987. 10.1089/ast.2009.0384.
8. Cornell, C.E., Black, R.A., Xue, M., Litz, H.E., Ramsay, A., Gordon, M., Mileant, A., Cohen, Z.R., Williams, J.A., Lee, K.K., et al. (2019). Prebiotic amino acids bind to and stabilize prebiotic fatty acid membranes. Proc Natl Acad Sci U S A *116*, 17239-17244. 10.1073/pnas.1900275116.
9. Black, R.A., Blosser, M.C., Stottrup, B.L., Tavakley, R., Deamer, D.W., and Keller, S.L. (2013). Nucleobases bind to and stabilize aggregates of a prebiotic amphiphile, providing a viable mechanism for the emergence of protocells. Proc Natl Acad Sci U S A *110*, 13272-13276. 10.1073/pnas.1300963110.
10. Szostak, J.W. (2011). An optimal degree of physical and chemical heterogeneity for the origin of life? Philosophical Transactions of the Royal Society B: Biological Sciences *366*, 2894-2901. 10.1098/rstb.2011.0140.
11. Imai, M., Sakuma, Y., Kurisu, M., and Walde, P. (2022). From Vesicles toward Protocells and Minimal Cells. Soft Matter. 10.1039/D1SM01695D.
12. Hargreaves, W.R., Mulvihill, S.J., and Deamer, D.W. (1977). Synthesis of phospholipids and membranes in prebiotic conditions. Nature *266*, 78-80.
13. Fiore, M., Madanamoothoo, W., Berlioz-Barbier, A., Maniti, O., Girard-Egrot, A., Buchet, R., and Strazewski, P. (2017). Giant vesicles from rehydrated crude mixtures containing unexpected mixtures of amphiphiles formed under plausibly prebiotic conditions. Org Biomol Chem *15*, 4231-4240. 10.1039/c7ob00708f.
14. Fiore, M., Chieffo, C., Lopez, A., Fayolle, D., Ruiz, J., Soulère, L., Oger, P., Altamura, E., Popowycz, F., and Buchet, R. (2022). Synthesis of Phospholipids Under Plausible Prebiotic Conditions and Analogies with Phospholipid Biochemistry for Origin of Life Studies. Astrobiology *22*, 598-627. 10.1089/ast.2021.0059.
15. Bonfio, C., Caumes, C., Duffy, C.D., Patel, B.H., Percivalle, C., Tsanakopoulou, M., and Sutherland, J.D. (2019). Length-Selective Synthesis of Acylglycerol-Phosphates through Energy-Dissipative Cycling. J Am Chem Soc *141*, 3934-3939. 10.1021/jacs.8b12331.
16. Budin, I., and Szostak, J.W. (2011). Physical effects underlying the transition from primitive to modern cell membranes. Proc. Nat. Acad. Sci. U.S.A. *108*, 5249-5254. 10.1073/pnas.1100498108.
17. Zhou, X., Dalai, P., and Sahai, N. (2020). Semipermeable Mixed Phospholipid-Fatty Acid Membranes Exhibit K(+)/Na(+) Selectivity in the Absence of Proteins. Life (Basel) *10*, 39. 10.3390/life10040039.
18. Fayolle, D., Altamura, E., D'Onofrio, A., Madanamothoo, W., Fenet, B., Mavelli, F., Buchet, R., Stano, P., Fiore, M., and Strazewski, P. (2017). Crude phosphorylation mixtures containing racemic lipid amphiphiles self-assemble to give stable primitive compartments. Scientific Reports *7*, 18106. 10.1038/s41598-017-18053-y.
19. Walde, P., Wessicken, M., Rädler, U., Berclaz, N., Conde-Frieboes, K., and Luisi, P.L. (1997). Preparation and Characterization of Vesicles from Mono-n-alkyl Phosphates and Phosphonates. The Journal of Physical Chemistry B *101*, 7390-7397. 10.1021/jp970898n.
20. Sarkar, S., Dagar, S., Lahiri, K., and Rajamani, S. (2022). pH-Responsive Self-Assembled Compartments

as Tuneable Model Protocellular Membrane Systems**. ChemBioChem *23*, e202200371. https://doi.org/10.1002/cbic.202200371.

21. Jordan, S.F., Rammu, H., Zheludev, I.N., Hartley, A.M., Maréchal, A., and Lane, N. (2019). Promotion of protocell self-assembly from mixed amphiphiles at the origin of life. Nature Ecology & Evolution *3*, 1705-1714. 10.1038/s41559-019-1015-y.
22. Rubio-Sánchez, R., O'Flaherty, D.K., Wang, A., Coscia, F., Petris, G., Di Michele, L., Cicuta, P., and Bonfio, C. (2021). Thermally Driven Membrane Phase Transitions Enable Content Reshuffling in Primitive Cells. Journal of the American Chemical Society *143*, 16589-16598. 10.1021/jacs.1c06595.
23. Steller, L.H., Van Kranendonk, M.J., and Wang, A. (2022). Dehydration Enhances Prebiotic Lipid Remodeling and Vesicle Formation in Acidic Environments. ACS Central Science *8*, 132-139. 10.1021/acscentsci.1c01365.
24. Fiore, M. (2018). The synthesis of mono-alkyl phosphates and their derivatives: an overview of their nature, preparation and use, including synthesis under plausible prebiotic conditions. Organic & Biomolecular Chemistry *16*, 3068-3086. 10.1039/C8OB00469B.
25. Gibard, C., Bhowmik, S., Karki, M., Kim, E.K., and Krishnamurthy, R. (2018). Phosphorylation, oligomerization and self-assembly in water under potential prebiotic conditions. Nat Chem *10*, 212-217. 10.1038/nchem.2878.
26. Toparlak, Ö.D., Karki, M., Egas Ortuno, V., Krishnamurthy, R., and Mansy, S.S. (2020). Cyclophospholipids Increase Protocellular Stability to Metal Ions. Small *16*, 1903381. 10.1002/smll.201903381.
27. Ortuno, V.E., Pulletikurti, S., Veena, K.S., and Krishnamurthy, R. (2022). Synthesis and hydrolytic stability of cyclic phosphatidic acids: implications for synthetic- and proto-cell studies. Chemical Communications *58*, 6231-6234. 10.1039/D2CC00292B.
28. Joyce, G.F., and Szostak, J.W. (2018). Protocells and RNA Self-Replication. Cold Spring Harb Perspect Biol *10*. 10.1101/cshperspect.a034801.
29. Gao, J., Huang, K., Zhang, X., Sun, Y., and Feng, S. (2018). Robust self-assembly properties of glyceryl decanoates synthesized under wetting and drying cycles. Gaodeng Xuexiao Huaxue Xuebao *39*, 849-854. 10.7503/cjcu20170857.
30. Apel, C.L., and Deamer, D.W. (2005). The Formation Of Glycerol Monodecanoate By A Dehydration Condensation Reaction: Increasing The Chemical Complexity Of Amphiphiles On The Early Earth. Origins of Life and Evolution of Biospheres *35*, 323-332. 10.1007/s11084-005-2046-8.
31. Maurer, S.E., and Nguyen, G. (2016). Prebiotic Vesicle Formation and the Necessity of Salts. Orig Life Evol Biosph *46*, 215-222. 10.1007/s11084-015-9476-8.
32. Monnard, P.-A., Apel, C.L., Kanavarioti, A., and Deamer, D.W. (2002). Influence of Ionic Inorganic Solutes on Self-Assembly and Polymerization Processes Related to Early Forms of Life: Implications for a Prebiotic Aqueous Medium. Astrobiology *2*, 139-152. 10.1089/153110702601922 37.
33. Kua, J., and Bada, J. (2011). Primordial Ocean Chemistry and its Compatibility with the RNA World. Origins of Life and Evolution of Biospheres *41*, 1-6. 10.1007/s11084-011-9250-5.
34. Krissansen-Totton, J., Arney, G.N., and Catling, D.C. (2018). Constraining the climate and ocean pH of the early Earth with a geological carbon cycle model. Proc Natl Acad Sci U S A *115*, 4105-4110. 10.1073/pnas.1721296115.
35. Halevy, I., and Bachan, A. (2017). The geologic history of seawater pH. Science *355*, 1069-1071. 10.1126/science.aal4151.
36. Joshi, M.P., Samanta, A., Tripathy, G.R., and Rajamani, S. (2017). Formation and Stability of Prebiotically Relevant Vesicular Systems in Terrestrial Geothermal Environments. Life (Basel) *7*, 51. 10.3390/life7040051.
37. Giuliano, C.B., Cvjetan, N., Ayache, J., and Walde, P. (2021). Multivesicular Vesicles: Preparation and Applications. ChemSystemsChem *3*, e2000049. 10.1002/syst.202000049.
38. Kanicky, J.R., and Shah, D.O. (2003). Effect of Premicellar Aggregation on the pKa of Fatty Acid Soap Solutions. Langmuir *19*, 2034-2038. 10.1021/la020672y.
39. Wellen, B.A., Lach, E.A., and Allen, H.C. (2017). Surface pKa of octanoic, nonanoic, and decanoic fatty acids at the air–water interface: applications to atmospheric aerosol chemistry. Physical Chemistry Chemical Physics *19*, 26551-26558. 10.1039/C7CP04527A.
40. Apel, C.L., Deamer, D.W., and Mautner, M.N. (2002).

Self-assembled vesicles of monocarboxylic acids and alcohols: conditions for stability and for the encapsulation of biopolymers. Biochim Biophys Acta *1559*, 1-9. http://dx.doi.org/10.1016/S0005-2736(01)00400-X.

41. Namani, T., and Walde, P. (2005). From Decanoate Micelles to Decanoic Acid/Dodecylbenzenesulfonate Vesicles. Langmuir *21*, 6210-6219. 10.1021/la047028z.

42. Toparlak, O.D. (2019). Mimics of Protocellular and Extant Life. Ph.D. Thesis, CIBIO departments, Univesrity of Trento, Trento, Italy. https://dx.doi.org/10.15168/11572_243297.

43. Walde, P. (2010). Building artificial cells and protocell models: experimental approaches with lipid vesicles. Bioessays *32*. 10.1002/bies.200900141.

44. Hanczyc, M.M., and Szostak, J.W. (2004). Replicating vesicles as models of primitive cell growth and division. Current Opinion in Chemical Biology *8*, 660-664. https://doi.org/10.1016/j.cbpa.2004.10.002.

45. Zhu, T.F., and Szostak, J.W. (2009). Preparation of large monodisperse vesicles. PLoS ONE *4*. 10.1371/journal.pone.0005009.

46. Zhu, T.F., Budin, I., and Szostak, J.W. (2013). Chapter Twenty - Preparation of Fatty Acid or Phospholipid Vesicles by Thin-film Rehydration. In Methods in Enzymology, J. Lorsch, ed. (Academic Press), pp. 267-274. https://doi.org/10.1016/B978-0-12-420067-8.00020-9.

47. Hughes, L.D., Rawle, R.J., and Boxer, S.G. (2014). Choose Your Label Wisely: Water-Soluble Fluorophores Often Interact with Lipid Bilayers. PLOS ONE *9*, e87649. 10.1371/journal.pone.0087649.

48. Fonteijn, T.A.A., Hoekstra, D., and Engberts, J.B.F.N. (1992). Vesicle formation of di-n-alkyl phosphates: liquid crystalline behavior, myelinization, counterion influence, and stability. Langmuir *8*, 2437-2447. 10.1021/la00046a016.

49. Dalai, P., Ustriyana, P., and Sahai, N. (2018). Aqueous magnesium as an environmental selection pressure in the evolution of phospholipid membranes on early earth. Geochimica et Cosmochimica Acta *223*, 216-228. https://doi.org/10.1016/j.gca.2017.11.034.

50. Jin, L., Kamat, N.P., Jena, S., and Szostak, J.W. (2018). Fatty Acid/Phospholipid Blended Membranes: A Potential Intermediate State in Protocellular Evolution. Small *14*, 1704077. https://doi.org/10.1002/smll.201704077.

51. O'Flaherty, D.K., Kamat, N.P., Mirza, F.N., Li, L., Prywes, N., and Szostak, J.W. (2018). Copying of Mixed-Sequence RNA Templates inside Model Protocells. J Am Chem Soc *140*, 5171-5178. 10.1021/jacs.8b00639.

52. Alsop, R.J., Maria Schober, R., and Rheinstädter, M.C. (2016). Swelling of phospholipid membranes by divalent metal ions depends on the location of the ions in the bilayers. Soft Matter *12*, 6737-6748. 10.1039/C6SM00695G.

53. Maurer, S. (2017). The Impact of Salts on Single Chain Amphiphile Membranes and Implications for the Location of the Origin of Life. Life (Basel) *7*, 44. 10.3390/life7040044.

54. Hunter, D.G., and Frisken, B.J. (1998). Effect of Extrusion Pressure and Lipid Properties on the Size and Polydispersity of Lipid Vesicles. Biophysical Journal *74*, 2996-3002. https://doi.org/10.1016/S0006-3495(98)78006-3.

55. Guo, Z., Hauser, N., Moreno, A., Ishikawa, T., and Walde, P. (2011). AOT vesicles as templates for the horseradish peroxidase-triggered polymerization of aniline. Soft Matter *7*, 180-193. 10.1039/C0SM00599A.

56. Guo, Z., Rüegger, H., Kissner, R., Ishikawa, T., Willeke, M., and Walde, P. (2009). Vesicles as Soft Templates for the Enzymatic Polymerization of Aniline. Langmuir *25*, 11390-11405. 10.1021/la901510m.

57. Namani, T., Ishikawa, T., Morigaki, K., and Walde, P. (2007). Vesicles from docosahexaenoic acid. Colloids and Surfaces B: Biointerfaces *54*, 118-123. https://doi.org/10.1016/j.colsurfb.2006.05.022.

58. Toparlak, Ö.D., Wang, A., and Mansy, S.S. (2021). Population-Level Membrane Diversity Triggers Growth and Division of Protocells. JACS Au *1*, 560-568. 10.1021/jacsau.0c00079.

59. Kristensen, K., Henriksen, J.R., and Andresen, T.L. (2014). Quantification of leakage from large unilamellar lipid vesicles by fluorescence correlation spectroscopy. Biochimica et Biophysica Acta (BBA) - Biomembranes *1838*, 2994-3002. https://doi.org/10.1016/j.bbamem.2014.08.007.

60. Mansy, S.S., and Szostak, J.W. (2008). Thermostability of model protocell membranes. Proc Natl Acad Sci U S A *105*. 10.1073/pnas.0805086105.

61. Goñi, F.M., and Alonso, A. (1999). Structure and functional properties of diacylglycerols in membranes1This work is

dedicated to Professor Vittorio Luzzati on occasion of his 75th birthday.1. Progress in Lipid Research *38*, 1-48. https://doi.org/10.1016/S0163-7827(98)00021-6.

62. Lo, S.-K., Tan, C.-P., Long, K., Yusoff, M.S.A., and Lai, O.-M. (2008). Diacylglycerol Oil—Properties, Processes and Products: A Review. Food and Bioprocess Technology *1*, 223-233. 10.1007/s11947-007-0049-3.

63. Serrallach, E.N., Dijkman, R., de Haas, G.H., and Shipley, G.G. (1983). Structure and thermotropic properties of 1,3-dipalmitoyl-glycero-2-phosphocholine. Journal of Molecular Biology *170*, 155-174. https://doi.org/10.1016/S0022-2836(83)80231-9.

64. Zumbuehl, A., Dobner, B., and Brezesinski, G. (2014). Phase behavior of selected artificial lipids. Current Opinion in Colloid & Interface Science *19*, 17-24. https://doi.org/10.1016/j.cocis.2014.01.003.

65. Rao, M., Eichberg, J., and Oro, J. (1982). Synthesis of phosphatidylcholine under possible primitive earth conditions. Journal of Molecular Evolution *18*, 196-202.

66. Rao, M., Eichberg, J., and Oro, J. (1987). Synthesis of phosphatidylethanolamine under possible primitive Earth conditions. Journal of Molecular Evolution *25*, 1-6.

67. Austin, S.M., and Waddell, T.G. (1999). Prebiotic Synthesis of Vitamin B6-type Compounds. Origins of life and evolution of the biosphere *29*, 287-296. 10.1023/A:1006532518221.

68. Miller, S.L., and Schlesinger, G. (1993). Prebiotic syntheses of vitamin coenzymes: I. Cysteamine and 2-mercaptoethanesulfonic acid (coenzyme M). Journal of Molecular Evolution *36*, 302-307.

69. Aleksandrova, M., Rahmatova, F., Russell, D.A., and Bonfio, C. (2023). Ring Opening of Glycerol Cyclic Phosphates Leads to a Diverse Array of Potentially Prebiotic Phospholipids. Journal of the American Chemical Society. 10.1021/jacs.3c07319.

70. Toparlak, Ö.D., Sebastianelli, L., Egas Ortuno, V., Karki, M., Xing, Y., Szostak, J.W., Krishnamurthy, R., and Mansy, S.S. (2023). Cyclophospholipids Enable a Protocellular Life Cycle. ACS Nano *17*, 23772-23783. 10.1021/acsnano.3c07706.

71. Kahana, A., Segev, L., and Lancet, D. (2023). Attractor dynamics drives self-reproduction in protobiological catalytic networks. Cell Reports Physical Science *4*, 101384. https://doi.org/10.1016/j.xcrp.2023.101384.

72. Mansy, S.S., Schrum, J.P., Krishnamurthy, M., Tobe, S., Treco, D.A., and Szostak, J.W. (2008). Template-directed synthesis of a genetic polymer in a model protocell. Nature *454*, 122-125.

73. Xue, M., Black, R.A., Cornell, C.E., Drobny, G.P., and Keller, S.L. (2020). A Step toward Molecular Evolution of RNA: Ribose Binds to Prebiotic Fatty Acid Membranes, and Nucleosides Bind Better than Individual Bases Do. Chembiochem *21*, 2764-2767. 10.1002/cbic.202000260.

74. Todd, Z.R., Cohen, Z.R., Catling, D.C., Keller, S.L., and Black, R.A. (2022). Growth of Prebiotically Plausible Fatty Acid Vesicles Proceeds in the Presence of Prebiotic Amino Acids, Dipeptides, Sugars, and Nucleic Acid Components. Langmuir *38*, 15106-15112. 10.1021/acs.langmuir.2c02118.

75. Lancet, D. (2014). Composomes. In Encyclopedia of Astrobiology, R. Amils, M. Gargaud, J. Cernicharo Quintanilla, H.J. Cleaves, W.M. Irvine, D. Pinti, and M. Viso, eds. (Springer Berlin Heidelberg), pp. 1-2. 10.1007/978-3-642-27833-4_5133-2.

76. Ruiz-Mirazo, K., Briones, C., and de la Escosura, A. (2014). Prebiotic systems chemistry: new perspectives for the origins of life. Chem Rev *114*, 285-366. 10.1021/cr2004844.